High Precision U–Pb Zircon Ages for Mesozoic Igneous Rocks from Hong Kong

R. J. Sewell[a], D. W. Davis[b] and S. D. G. Campbell[a,1]

[a]Geotechnical Engineering Office, Civil Engineering and Development Department, 101 Princess Margaret Road, Kowloon, Hong Kong Special Administrative Region, China.
[b]Jack Satterly Geochronology Laboratory, Department of Geology, University of Toronto, Toronto, Ont., Canada.

Abstract: Sixteen new high precision U–Pb zircon ages are reported from Jurassic and Early Cretaceous silicic volcanic and plutonic rocks of Hong Kong. When combined with the existing age dataset, the new ages constrain more tightly the timing of major periods of volcanism and plutonism at 162.6 ± 4.5 Ma, 146.7 ± 1.1 Ma, 143.0 ± 1.0 Ma and 140.8 ± 0.6 Ma. However, two ages of 151.9 ± 0.2 Ma and 148.1 ± 0.2 Ma, from eastern New Territories and southern Hong Kong indicate additional and therefore more continuous, albeit pulsed, magmatic activity than previously thought.

Keywords: Hong Kong, U–Pb dating, Mesozoic, zircon

1. Introduction and Geological Setting

Jurassic to Cretaceous silicic volcanic rocks and related granitoid rocks crop out over approximately 85% of the land surface area of the Hong Kong Special Administrative Region (1050 km^2, herein called Hong Kong). They belong to a 400 km wide belt of Mesozoic (Yanshanian) magmatic rocks exposed along the coastal region of southeast China and have been divided into four main volcanic groups, and corresponding granitoid suites, based on petrographic, geochemical and age criteria (Davis et al., 1997; Sewell et al., 2000; Campbell et al., 2007). The spatial distribution and geometry of the volcanic centers and related plutons in Hong Kong are strongly controlled by east-, north-, northwest- and northeast-trending faults (Figs. 1– 4). These faults are thought to have been active during periods of

1 Present Address: British Geological Survey, Murchison House, Edinburgh EH9 3LA, United Kingdom.

rapid, pulsed, crustal extension with associated strike-slip movement along the northeast-trending Lianhuashan Fault Zone during the Late Mesozoic (Campbell and Sewell, 1997).

This paper presents new U–Pb zircon dates on volcanic rocks, dykes and granitoid plutons from each of the four magmatic groups measured by isotope dilution thermal ionization mass spectrometry (ID-TIMS) (Table 1). Samples were collected in order to further refine knowledge of the pace and episodicity of magmatism. Details of sample locations and field relationships are given in Table 1 and Figs 2–4.

2. Analytical Methods

2.1 Laboratory Procedures

Rocks were crushed with a jaw crusher followed by a disk mill. Initial separation involved multiple passes of crushed rock over a Wilfley table to concentrate heavy minerals. Further heavy mineral separation was carried out by density separations with bromoform and methylene iodide and paramagnetic separations with a Frantz isodynamic separator. Descriptions of zircon populations are given in Table 1. Final sample selection was by hand picking under a microscope, choosing the freshest, least-cracked zircon grains. In some cases, exterior surfaces of selected zircon grains were removed by air abrasion (AA, Krogh 1982). In others, zircon populations were treated by the chemical abrasion (CA, Mattinson, 2005) method. Zircon grains that underwent CA treatment were annealed in quartz crucibles at 1000ºC for 3 days. This removes much, although not all, of the radiation damage induced by decay of U and Th contained in the mineral, rendering the unmetamict zircon more inert to chemical attack. The annealed grains were subsequently leached in a 1:1 mixture of concentrated HF and 6N HCl for about 16 hours in a teflon bomb at 195ºC. The metamict and altered parts of the crystals, which contain isotopically disturbed Pb, dissolve more rapidly than annealed, unaltered crystal domains for low to moderate levels of radiation damage.

Attack was variable, depending on the uranium concentration of the grains and the consequent degree of radiation damage. Residues of damaged grains consist of whitish fragments. Fragments were chosen to contain as little white discoloration as possible. In cases where there is noticeable etching, the presence of a small amount of discolouration does not seem to affect the results.

To minimise the possibility of inheritance, a minimum number of zircon grains was analyzed in a fraction having characteristics typical of the igneous population, such as a euhedral shape and an abundance of melt or rod-like inclusions. Weights of mineral fractions chosen for ID-TIMS analysis were estimated from photomicrographs (Matthews and Davis, 1999). Estimated weights should be accurate to about ±20%. This affects only U and Pb concentrations, not age information, which depends only on isotope ratio measurements (Table 2). Samples were washed briefly in HNO_3 prior to dissolution. For AA grains, ^{205}Pb-^{235}U spike was added to the dissolution capsules during sample loading. In the case of CA grains, ^{205}Pb-^{233}U -^{235}U spike was added after HF dissolution.

Zircon grains were dissolved using concentrated HF in teflon bombs at 195^{o}C for 5 days, then redissolved in 3N HCl to ensure equilibration with the spike (Krogh, 1973). U and Pb were separated using 0.05 ml anion exchange columns.

Pb and UO_2 were analyzed on a VG354 mass spectrometer using a Daly collector in pulse counting mode for small samples. The mass discrimination correction for this detector is constant at 0.07%/AMU. Larger samples were analyzed in multidynamic mode using 3 high mass Faraday collectors and the axial Daly detector. The Daly gain was continually monitored by measuring the ^{205}Pb signal in the Daly and adjacent Faraday collectors. Thermal mass discrimination corrections are 0.10% /AMU for Pb. For CA samples, mass discrimination for U was corrected using measured $^{233}UO_2$ /$^{235}UO_2$ ratios after correction for O isotopic composition. Dead time of the Daly system (about 20 nsec) and multi-collector

Faraday cup efficiencies were monitored using the SRM982 Pb standard. Faraday amplifier gains were monitored daily using a constant current source.

2.2 Data analysis

Isotope results are given in Table 2 as ages with 2σ absolute errors. Concordia coordinates and errors are readily calculated from the ages using formulas given in the footnotes to Table 2. Average ages are summarized in Table 3 (errors here and in the text are given at 95% confidence). Data from individual samples are presented as 2σ error ellipses on concordia plots on Figs 5–8. Mass spectrometer data were reduced using in-house software (UTILAge program written by D.W. Davis). Age results were averaged and plotted on concordia diagrams using Isoplot software (Ludwig, 2003). U decay constants are from Jaffey et al. (1971). Probability of fit is a measure of the likelihood that data overlap within error. In a random distribution of coeval data with correctly assigned errors, this would be expected to be 50% on average. Low values generally indicate scatter due to Pb loss or inheritance.

Common Pb corrections are made assuming an isotopic composition similar to laboratory blank. The plotted data, as well as results in Tables 2 and 3, are corrected for ^{230}Th disequilibrium, assuming a Th/U ratio in the magma of 4.2, the terrestrial average. This increases the ^{206}Pb/^{238}U ages by about 0.09 Ma in all of the samples. Th/U is calculated from the measured ^{208}Pb/^{206}Pb ratio and ^{206}Pb/^{238}U age.

Because of depletion of the shorter half-life ^{235}U isotope, there is much less ^{207}Pb than ^{206}Pb for relatively young samples. Therefore, for Mesozoic and younger samples, ^{206}Pb/^{238}U ages are much more precise and reliable than ^{207}Pb/^{235}U ages, which are subject to greater corrections for common Pb, as well as possible measurement biases and excess ^{207}Pb from disequilibrium values of ^{231}Pa. A bias from one or more of these sources is the likely reason why many of the error ellipses plot slightly to the right of the concordia curve. Discordance may also be due in part to a systematic error in the ^{235}U decay constant as suggested by Schoene et al. (2006). $^{207}Pb/^{206}Pb$ ages are quite imprecise because the concordia curve is nearly parallel to a line through the origin. Therefore, ages for these samples are calculated as $^{206}Pb/^{238}U$ ages. $^{206}Pb/^{238}U$ ages are sensitive to secondary Pb loss, but this is likely to have been eliminated by the AA and CA treatments.

3. Results

Samples in Tables 1-3 and Figs 5-8 are grouped according to age. Most samples produced overlapping data sets with clearly defined ages. Slight indications of inheritance in samples HK12067, HK13277 and HK13278 may be due to cores or zircon xenocrysts from earlier events. The measured age range of inheritance is less than a million years so it may be due to cores from earlier phases of magmatism making up the same event or 'autocrysts' from earlier pulses of magmatism within the same magma chamber. In these cases, multiple analyses were carried out and the eruptive age was estimated from the average of the youngest cluster of overlapping data. HK12073 shows inheritance from a Paleoproterozoic source (from the ca. 1850 Ma projection of a discordant datum, Fig. 8d). Zircon analyzed from HK9015 may all be inherited from a variety of Phanerozoic sources (Fig 7d). In this case, only an older age limit can be defined.

Despite the above complications, at least four distinct short-lived periods of magmatism can be recognized. Taking the mean and twice the standard deviation of ages from periods 1 to 4, respectively, gives 162.5 ± 4.7 Ma (2 samples) for Period 1, 146.9 ± 1.6 Ma (5 samples) for Period 2, 143.1 ± 1.2 Ma (4 samples) for Period 3, and 140.9 ± 0.6 Ma (4 samples) for Period 4. One age of 151.9 ± 0.2 Ma was not included since it falls outside the apparent duration of ca. 3 Ma for the closest period.

Each of the periods, except the first, contains multiple samples with overlapping ages that may allow magmatic ages to be defined to a higher level of precision than previously defined. The youngest data clusters from three samples from Period 2 give overlapping ages. If it is assumed that all three samples crystallized at the same time, a more precise age for this event of 146.37 ± 0.08 Ma (73% probability of fit over 10 data) can be obtained by pooling the data. Similarly, eight overlapping data from three samples in Period 3 give 142.96 ± 0.13 Ma (61% probability of fit), while eleven data from three samples in Period 4 overlap with an average age of 140.73 ± 0.15 Ma (60% probability of fit). However, it should be emphasized that these ages and errors are only meaningful if the samples from each group are coeval.

4. Discussion

The analyzed samples add significantly to the already substantial existing age dataset arising from previous stratigraphical, geochronological and geochemical studies on the volcanic and plutonic rocks of Hong Kong (Campbell and Sewell, 1997; Davis et al., 1997; Sewell et al., 2000; Campbell et al., 2007; Table 3). As a result, all of the fifteen Middle Jurassic to Early Cretaceous volcanic formations recognized in Hong Kong have now been precisely dated using U–Pb single crystal zircon geochronology. Among the intrusive rocks, twenty-one of the twenty-five recognized units (Sewell et al., 2000) have now been radiometrically dated. These include several plutons that occur only on outlying islands, and several rhyolite dyke swarms (Figs 2 and 3). In addition, the ages of several isolated volcanic outcrops (Fig. 4), previously correlated only on the basis of whole-rock geochemistry, have now been confirmed. The exceptionally tightly-constrained record of Mesozoic volcanic and plutonic activities provided by the precise zircon ages reveal, in remarkable detail, the cyclic nature of Late Yanshanian magmatism in this comparatively small area.

Campbell and Sewell (1997) demonstrated that eastnortheast-trending and northwest-trending faults exerted a strong influence on the distribution and loci of Middle Jurassic to Early Cretaceous volcanic deposits and centers in Hong Kong. They inferred that as the regional tectonic stress field changed from an active margin dominated by subduction to a back-arc regime dominated by crustal attenuation, dextral strike-slip movement along eastnortheast-trending faults gave way to sinistral strike-slip movement. This transition was accompanied by increasing activity on northwest-trending faults punctuated by periods of unusually rapid extension.

The oldest measured U–Pb age on the Sai Lau Kong Formation (HK12026, Fig. 4; Fig. 5a) places an upper limit of 164.1 Ma on the age of the Tsuen Wan Volcanic Group. Moreover, the presence of tuff-breccia and rhyodacite lava flows suggests that the formation occupies a northwest-trending depression related to a nearby volcanic fissure-vent. Therefore, the Sai Lau Kong Formation may mark the earliest expression of changes in the regional stress field leading to the onset of sinistral strike-slip fault movement and rapid extension in the Hong Kong area.

The 160.8 ± 0.2 Ma age of the Chek Mun Rhyolite (HK12069, Fig. 4; Fig. 5b) suggests that eastnortheast-trending and northeast-trending axes of extension and dextral transtension were dominant in the late Middle Jurassic (Campbell and Sewell, 1997). Sporadic northeast-trending rhyolite dykes also intrude the A-type Lamma Suite granitoids (Table 3) in the western New Territories dated at ca.159 Ma (Davis et al., 1997) suggesting that dextral transtension continued to dominate the regional structural regime at this time.

Previously, the only indication of magmatic activity outside the four distinct periods of Middle Jurassic to Lower Cretaceous magmatism in Hong Kong was from zircon inheritance (Davis et al., 1997), and these ages generally indicated Precambrian sources rather than broadly contemporaneous magmatism. However, rocks belonging to the 146 Ma period have consistently revealed inherited zircon ages of between 149.5 ± 0.4 Ma and 153.8 ± 0.4 Ma (Davis et al., 1997), suggesting that a latent igneous event may have occurred during this period. The new date from a rhyolite dyke (HK12066, Fig. 3; Fig. 6a) at the southern tip of D'Aguilar Peninsula confirms the presence of this magmatic event although it has no major volcanic expression within Hong Kong. Furthermore, the location of the dyke, close to the southern margin of Hong Kong, suggests that a magmatic province of that age could lie immediately to the south of Hong Kong waters.

The 148.1 ± 0.2 Ma age on the South Lamma Granite (HK 12075, Fig. 3; Fig. 6b) is slightly older than the oldest age so far recognized for the ca.146 million year old magmatic period. The stratigraphically lowermost volcanic rocks belonging to the Lantau Volcanic Group on Lantau Island have been dated at 147.5 ± 0.2 Ma (Campbell et al., 2007; Table 3), whereas the bulk of the volcanic and intrusive rocks within the Group and the coeval subvolcanic Kwai Chung Suite have been dated at 146.4 ± 0.2 Ma (Davis et al., 1997; Table 3). Geochemically, the South Lamma Granite is similar to granites belonging to the Kwai Chung Suite, although prior to obtaining the new age it had been assigned to the Cheung Chau Suite (Table 3) largely on the basis of petrographic criteria. Thus, the best interpretation for the South Lamma Granite is that it belongs to an early phase of emplacement of the Kwai Chung Suite. The 147.3 ± 0.2 Ma age for a swarm of east–west-trending rhyodacite dykes (Shan Tei Tong Rhyodacite, HK13273, Fig. 3; Fig. 6c) intruding the South Lamma Granite suggests that these dykes may signal the onset of rapid extension that characterised the main ca.146 million year old magmatic period.

A U–Pb zircon age of 146.2 ± 0.2 Ma had previously been obtained for a sample of the Sha Tin Granite (Davis et al., 1997; Table 3) collected from north of the Tolo Channel Fault. Two samples of granite collected from south of the Tolo Channel Fault have now revealed evidence for two separate intrusions. The 146.4 ± 0.1 Ma age of coarse-grained granite (HK13278, Fig. 2; Fig. 6d) from north of Kowloon reveals that it belongs to the Sha Tin Granite. By contrast, the new 144.0 ± 0.3 Ma age for medium-grained granite (HK12072, Fig. 2; Fig. 7a) from northeast of Kowloon has confirmed the existence of a northeast-oriented ellipsoidal pluton (Shui Chuen O Granite) belonging to the Period 3 magmatic event. Previously, the only dated granite pluton belonging to this event (Davis et al., 1997; Table 3) was known from Chi Ma Wan farther to the southwest. The new age indicates that plutonism belonging to the ca. 143 Ma event is more widespread and voluminous than previously thought.

A new age has now been obtained for medium-grained granite on the Po Toi Islands (HK13274, Fig. 3; Fig. 6e), which was previously assigned to the 141 Ma event. The new 146.4 ± 0.2 Ma age for the granite confirms, however, that it was emplaced earlier during Period 2 magmatism. This suggests that a major east–west-trending magnetic anomaly lying to the south of the Stanley and Lamma peninsulas may represent a major tectonomagmatic discontinuity.

The 146.4 ± 0.2 Ma age of the feldspar-phyric rhyolite dyke (HK13269, Fig. 2; Fig. 6f) from the island of Kau Yi Chau in Victoria Harbour indicates that it belongs to an easterly extension of the Lantau Dyke swarm previously dated at 146.3 ± 0.3 (Davis et al., 1997; Table 3). A small outcrop of coarse ash crystal tuff on Kau Yi Chau, which is cut by the dyke, most likely also belongs to the ca.164 Ma event.

The age of the Mount Davis Formation (HK13275, Fig. 2; Fig. 7b) at its type locality in northwest Hong Kong Island has now been confirmed. Previously, this formation was dated at 142.8 ± 0.2 Ma (Campbell et al., 2007; Table 3) based on a single sample from a distal outlier on Lantau Island. The new 143.0 ± 0.3 Ma age confirms that the bulk of the volcanic rocks forming Hong Kong Island belong to the ca.143 Ma magmatic event.

The 142.9 ± 0.2 Ma age for the sample of tuff from Mang Kung Uk Formation (HK12067, Fig. 2; Fig. 7c) confirms that it also belongs to the ca. 143 Ma Period 3 magmatic event. This volcaniclastic unit may have accumulated in a depression formed as a result of a caldera-forming eruption that deposited the underlying Che Kwu Shan Formation.

The <142.7 ± 0.1 Ma age of the sample of tuff from the Ngo Mei Chau Formation (HK9015, Fig. 4; Fig. 7d) confirms the observations of Lai et al. (1996) regarding the stratigraphy of this unit. The data are also in accord with available geochemical and petrographic data for the formation, indicating close similarities with the Ap Lei Chau Formation of the Repulse Bay Volcanic Group. Inheritance data yielded by this sample also support other recently acquired age data that indicate a thermal event at around 148 Ma (Campbell et al., 2007). As discussed earlier, this event may have been a precursor to the major period of volcanism and plutonism at 146 Ma (Davis et al., 1997), which was dominated by a northeast- to eastnortheast-trending structural regime.

The new 141.2 ± 0.3 Ma age for the Pan Long Wan Formation (HK13277, Fig. 2; Fig. 8a) suggests that it probably represents the first eruption of the Kau Sai Chau Volcanic Group. This trachydacite lava unit immediately overlies the Mang Kung Uk Formation and may represent a cryptodome that extruded prior to caldera-forming eruptions associated with the ca. 141 Ma Period 4 magmatic event. This age is also similar to one reported earlier for fine ash tuff of the Kau Sai Chau Volcanic Group (undifferentiated) from Lantau Island (Table 3, Campbell et al., 2007), which rests unconformably on the crystal tuff of the Repulse Bay Volcanic Group.

The overlapping 140.6 ± 0.3 Ma ages of quartz monzonite from D’Aguilar Peninsula (HK12022, Fig. 3; Fig. 8b) and the Sok Kwu Wan Granite (HK12023, Fig. 3; Fig. 8c) from Lamma Island indicate that they belong to the youngest period of volcanic and plutonic activity in Hong Kong, which was previously dated at 140.8 Ma (Davis et al., 1997).

Geochemical and petrographic similarities also suggest that these separate outcrops are distinct facies of the same intrusion. Outcrops of quartz monzonite in Hong Kong are generally related to ‘fissure-type’ plutonic-volcanic assemblages (Sewell and Campbell, 1997) that are thought to mark deep crustal fractures and caldera boundaries. The linear series of discontinuous quartz monzonite stocks across southern Hong Kong Island and Lamma Island are closely associated with screens of fine-grained granite that may represent more fractionated equivalents of the quartz monzonite.

The new 140.9 ± 0.2 Ma age for the large intrusion of flow-banded feldspar-phyric rhyolite at Shek Nga Shan (HK12073, Fig. 2; Fig. 8d) suggests that it probably fed lava flows of the Clear Water Bay Formation exposed farther east.

With the exception of the Hok Tsui Rhyolite, average $^{206}Pb/^{238}U$ ages for the different magmatic periods may be defined by combining all of the available U–Pb age data from previous studies (Table 3). These are: Period 1, 162.6 ± 4.5 Ma (11 samples); Period 2, 146.7 ± 1.1 Ma (13 samples); Period 3, 143.0 ± 1.0 Ma (10 samples); and Period 4, 140.8 ± 0.6 Ma (9 samples). It is noteworthy that the recurring periods of magmatism during the Middle Jurassic to Early Cretaceous show a general trend toward shorter and more energetic pulses with time, along with a narrowing of repose intervals. The catastrophic eruption of the High Island tuff (ca. 141 Ma) appears, therefore, to represent the final, cataclysmic expression of a string of magmatic pulses that surged in frequency and intensity toward the end of the Early Yanshanian (190–140 Ma) magmatic period in southeastern China.

5. Conclusions

Sixteen new precise U–Pb single zircon ages for intrusive rocks from southern Hong Kong lead to the following conclusions:

1) The new ages add significantly to the existing age dataset for Hong Kong and constrain more tightly the timing of major periods of volcanism and plutonism at 162.6 ± 4.5 Ma, 146.7 ± 1.1 Ma, 143.0 ± 1.0 Ma and 140.8 ± 0.6 Ma.

2) A previously unrecognized magmatic event in the Hong Kong region occurred 152 million years ago. Although as yet only one absolute zircon age for this event has been recorded, several previously dated samples from Hong Kong have revealed inheritance data from the same event. The preserved and exposed volcanic expression of this event appears, however, to be limited.

3) The main magmatic period at ca.146 Ma was preceded by a precursor magmatic pulse at 148 Ma, which may have signalled the onset of accelerated extensional tectonics. The new age for the South Lamma Granite also suggests that the east–west-trending rhyodacite dykes on Lamma Island belong to an early pulse of the Lantau Dyke Swarm.

4) The final period of magmatism at ca. 141 Ma commenced with extrusion of trachydacite magma prior to the onset of major explosive rhyolitic eruptions.

5) Stocks of quartz monzonite in southern Hong Kong between the D’Aguilar Peninsula and Lamma Island probably belong to the same intrusive unit. These stocks may mark the position of a major structural feature, possibly a caldera boundary at depth as quartz monzonites associated with later volcanic periods can be strong indicators of caldera-bounding faults (Campbell and Sewell, 1997).

6) Combined with structural data, these new ages provide further confirmation that northwest-trending and northeast- to eastnortheast-trending faults are likely to have exercised a strong influence on the distribution, loci and form of volcanic centers. Although dextral strike-slip movement on northeast- to eastnortheast-trending faults may have been dominant throughout the main periods of Middle Jurassic to Early Cretaceous magmatism, sinistral strike-slip movement, indicating changes in the regional tectonic stress field, seems to have commenced sporadically as early as the Middle Jurassic.

7) The new age data presented in this study indicate that Jurassic to Cretaceous magmatism in Hong Kong was mostly concentrated in at least four distinct episodes but activity also occurred sporadically between these periods.

Acknowledgements

Isotope work was carried out in the Jack Satterly Geochronology Laboratory at the Royal Ontario Museum, Toronto, Canada, and the Department of Geology, University of Toronto, with assistance from Y.Y. Kwok. We are grateful to F. Corfu and an anonymous reviewer for helpful comments which considerably improved the manuscript. This paper is published with the approval of the Director of Civil Engineering and Development, Hong Kong SAR, China. S.D.G. Campbell publishes with the permission of the Executive Director of the British Geological Survey, and thanks to Alison Monaghan for her review of the manuscript.

References

Campbell, S.D.G., Sewell, R.J., 1997. Structural control and tectonic setting of Mesozoic volcanism in Hong Kong. Journal of the Geological Society, London 154, 1039–1052

Campbell, S.D.G., Sewell, R.J., Davis, D.W., So, A.C.T., 2007 New U–Pb age and geochemical constraints on the stratigraphy and distribution of the Lantau Volcanic Group, Hong Kong. Journal of Asian Earth Sciences 31, 139–152.

Davis, D.W., Sewell, R.J., Campbell, S.D.G., 1997. U–Pb dating of Mesozoic igneous rocks from Hong Kong. Journal of the Geological Society, London 154, 1067–1076.

Jaffey, A.H., Flynn, K.F., Glendenin, L.E., Bentley, W.C., Essling, A.M., 1971. Precision measurement of half-lives and specific activities of ^{235}U and ^{238}U. Physical Review 4, 1889–1906.

Krogh, T.E., 1973. A low contamination method for hydrothermal decomposition of zircon and extraction of U and Pb for isotopic age determinations. Geochimica et Cosmochimica Acta 37, 485–494.

Krogh, T.E., 1982. Improved accuracy of U–Pb ages by the creation of more concordant systems using an air abrasion technique. Geochimica et Cosmochimica Acta 46, 637–649.

Lai, K.W., Campbell, S.D.G., Shaw, R., 1996. Geology of the northeastern New Territories. Hong Kong Geological Survey Memoir No. 5. Geotechnical Engineering Office, Hong Kong.

Ludwig, K.R., 2003. User's manual for Isoplot 3.00 a geochronological toolkit for Excel. Berkeley Geochronological Center Special Publication 4.

Matthews, W., Davis, W.J., 1999. A practical image analysis technique for estimating the weight of abraded mineral fractions used in U-Pb dating, in: Radiogenic Age and Isotopic Studies: Report 12; Geological Survey of Canada, Current Research 1999-F, pp. 1–7.

Mattinson, J., 2005. Zircon U-Pb chemical abrasion (CA-TIMS) method: Combined annealing and multi-step partial dissolution analysis for improved precision and accuracy of zircon ages. Chemical Geology, 220, 47–66.

Schoene, B., Crowley, J.L., Condon, D.J., Schmitz, M.D. and Bowring, S.A., 2006. Reassessment of uranium decay constants for geochronology using ID-TIMS UPb data. Geochimica et Cosmoachimica Acta, 70,: 426-445.

Sewell, R.J., Campbell, S.D.G., 1997. Geochemistry of coeval Mesozoic plutonic and volcanic suites in Hong Kong. Journal of the Geological Society, London 154, 1053–1066.

Sewell, R.J., Campbell, S.D.G., Fletcher, C.J.N., Lai, K.W., Kirk, P.A., 2000. The Pre-Quaternary Geology of Hong Kong. Geotechnical Engineering Office, Civil Engineering Department, The Government of the Hong Kong Special Administrative Region.

Figure Captions

Figure 1. Simplified geological map of Hong Kong showing distribution of Middle Jurassic to Early Cretaceous volcanic–plutonic groups, general location of dated samples, and regional geological setting.

Figure 2. Simplified geological map of northern Hong Kong, Kowloon, and central New Territories showing the location of analyzed samples, outcrop of relevant volcanic and plutonic units, and major structural features (refer to Table 3 for key to abbreviations).

Figure 3. Simplified geological map of southern Hong Kong showing the location of analyzed samples, outcrop of relevant intrusive units, and major structural features (refer to Table 3 for key to abbreviations).

Figure 4. Simplified geological map of NE New Territories showing the location of analyzed samples, outcrop of relevant volcanic formations, and major structural features (refer to Table 3 for key to abbreviations).

Figure 5. U–Pb concordia plots for Jurassic rocks of Period 1.

Figure 6. U–Pb Concordia plots for Late Jurassic rocks of Period 2 and the Hok Tsui Rhyolite dyke, which may be representative of a slightly earlier period of magmatism responsible for inherited zircon.

Figure 7. U–Pb concordia plots for Cretaceous magmatism of Period 3.

Figure 8. U–Pb concordia plots for Cretaceous magmatism of Period 4.

Figure 1 Print Only

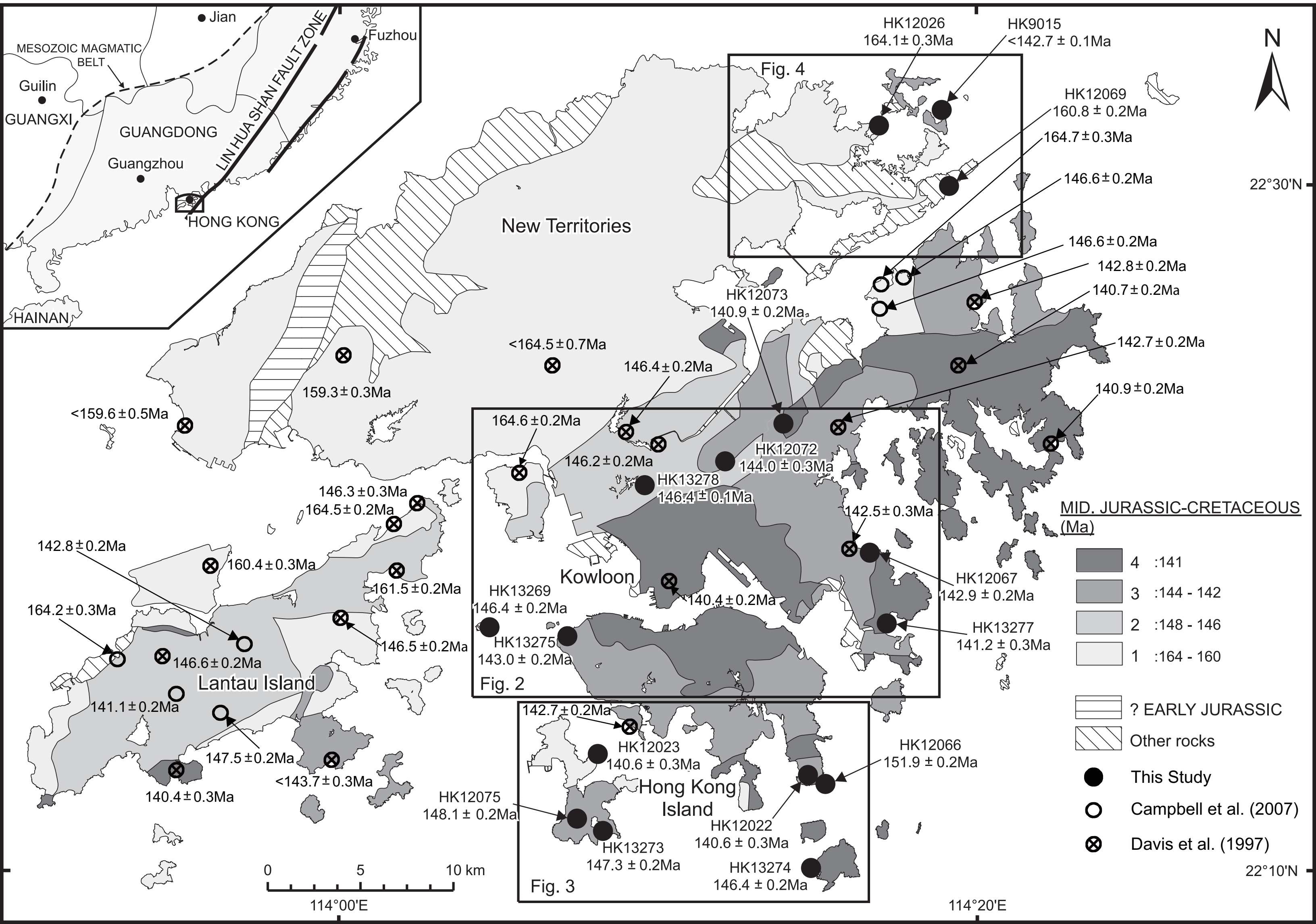

Figure 1 Web Only

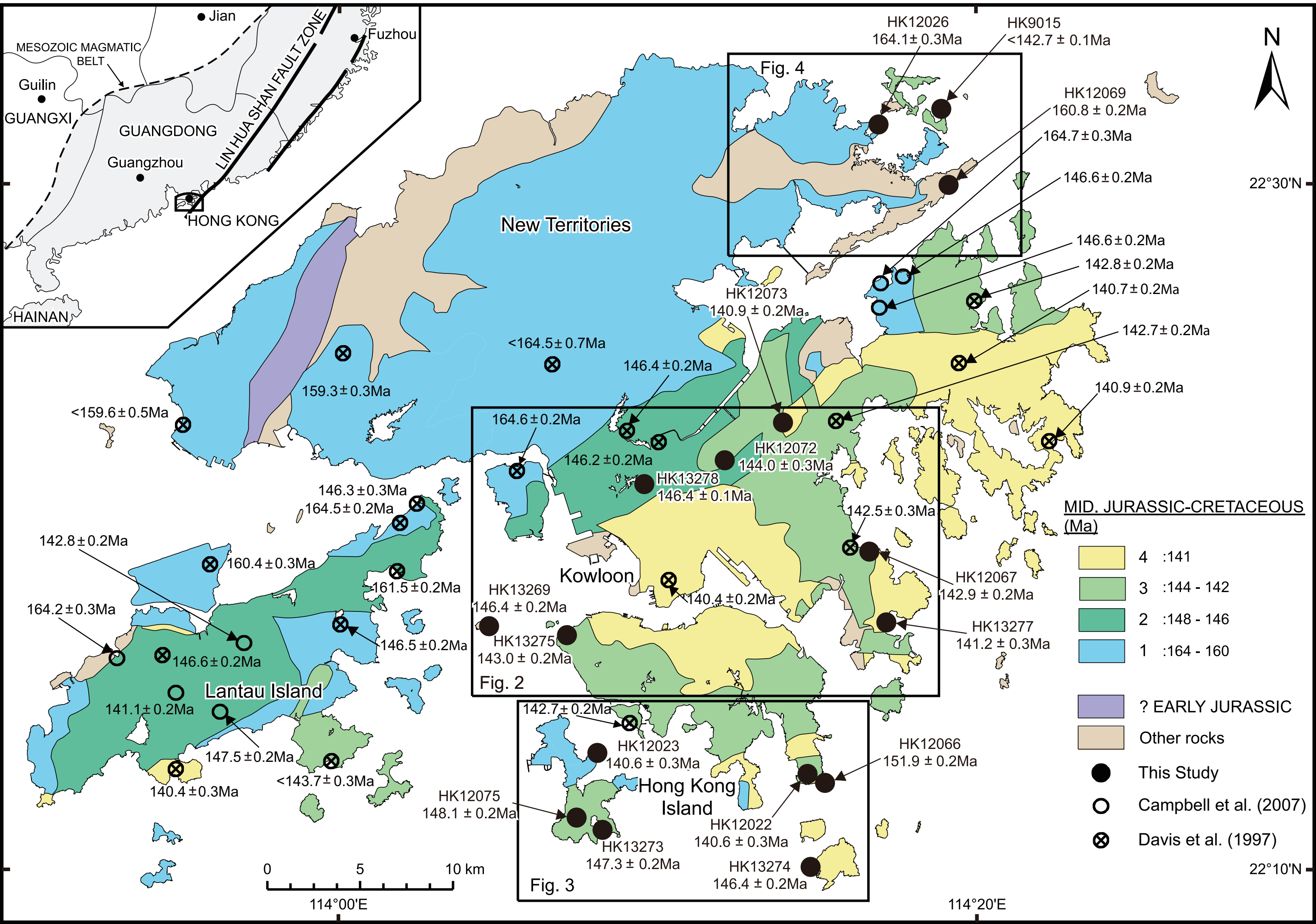

Figure 2 Print Only

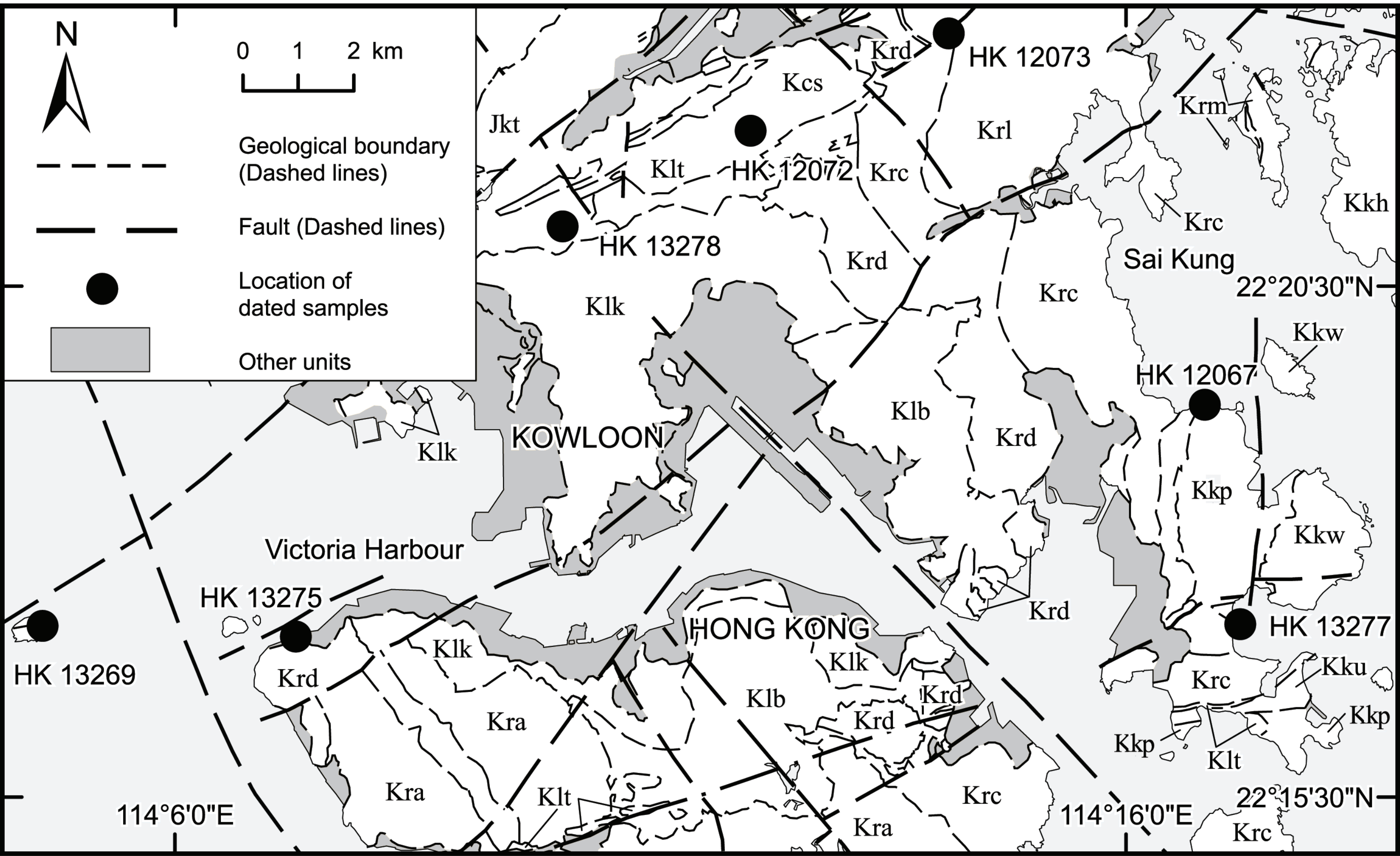

Figure 2 Web Only

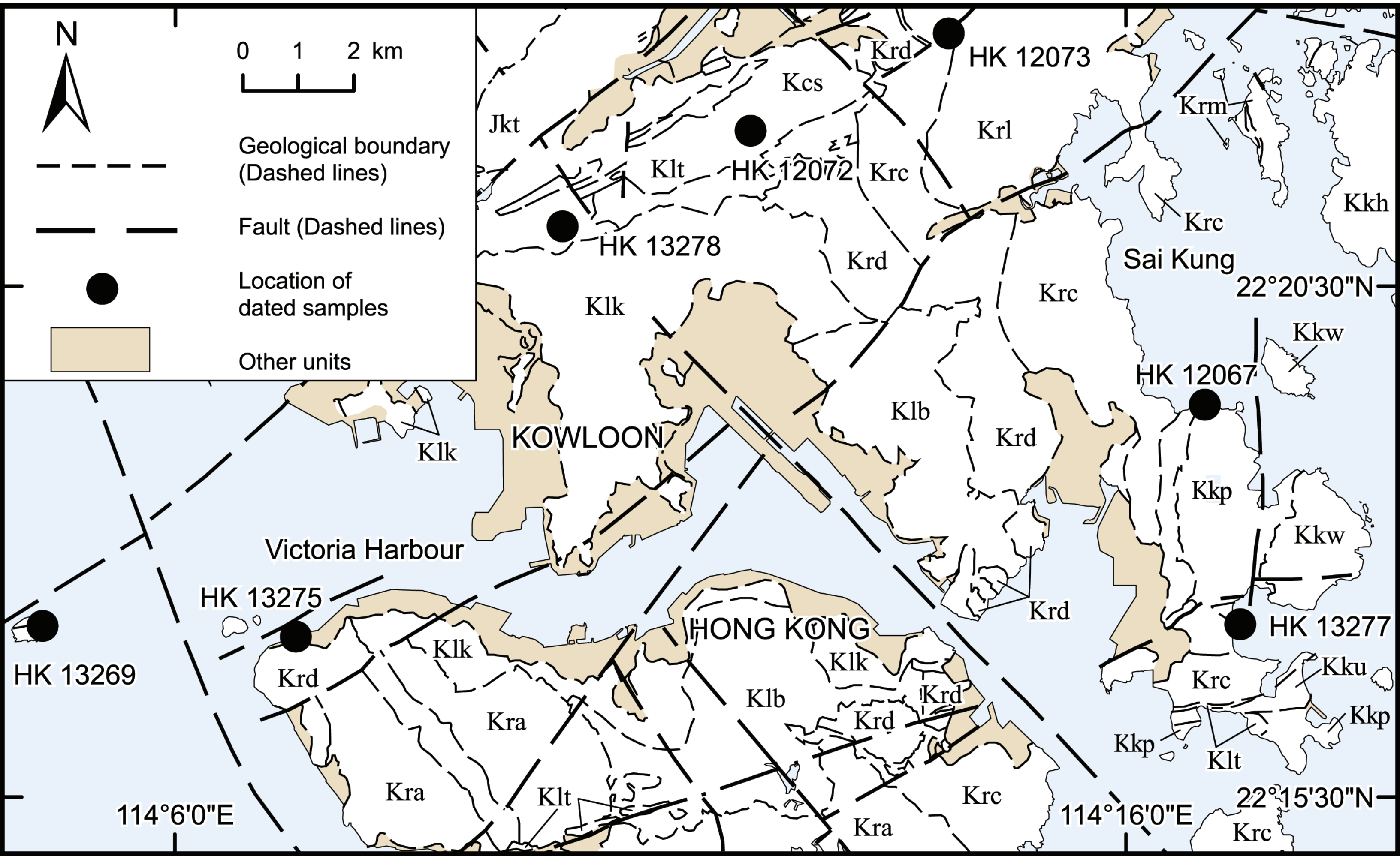

Figure 3 Print Only

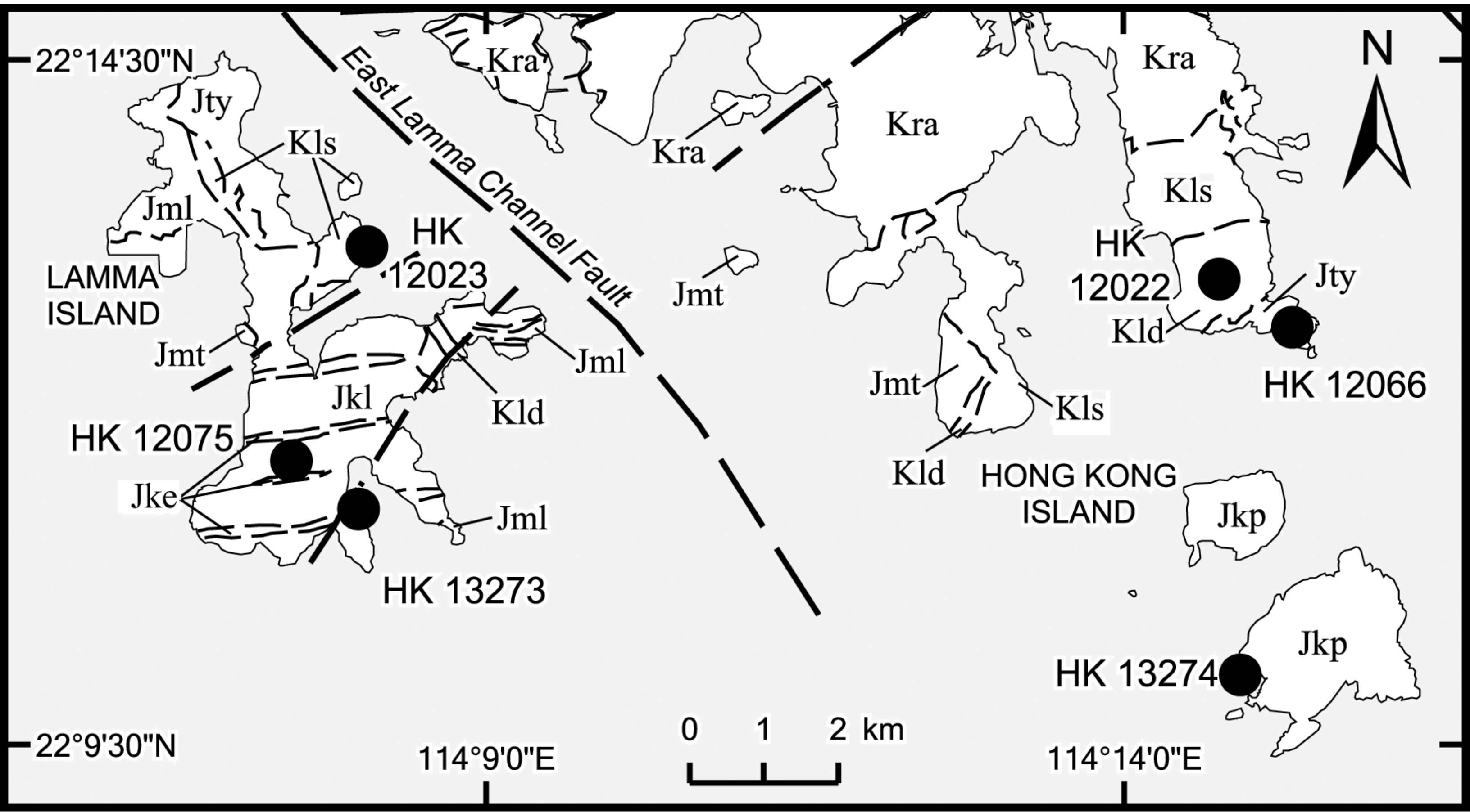

Figure 3 Web Only

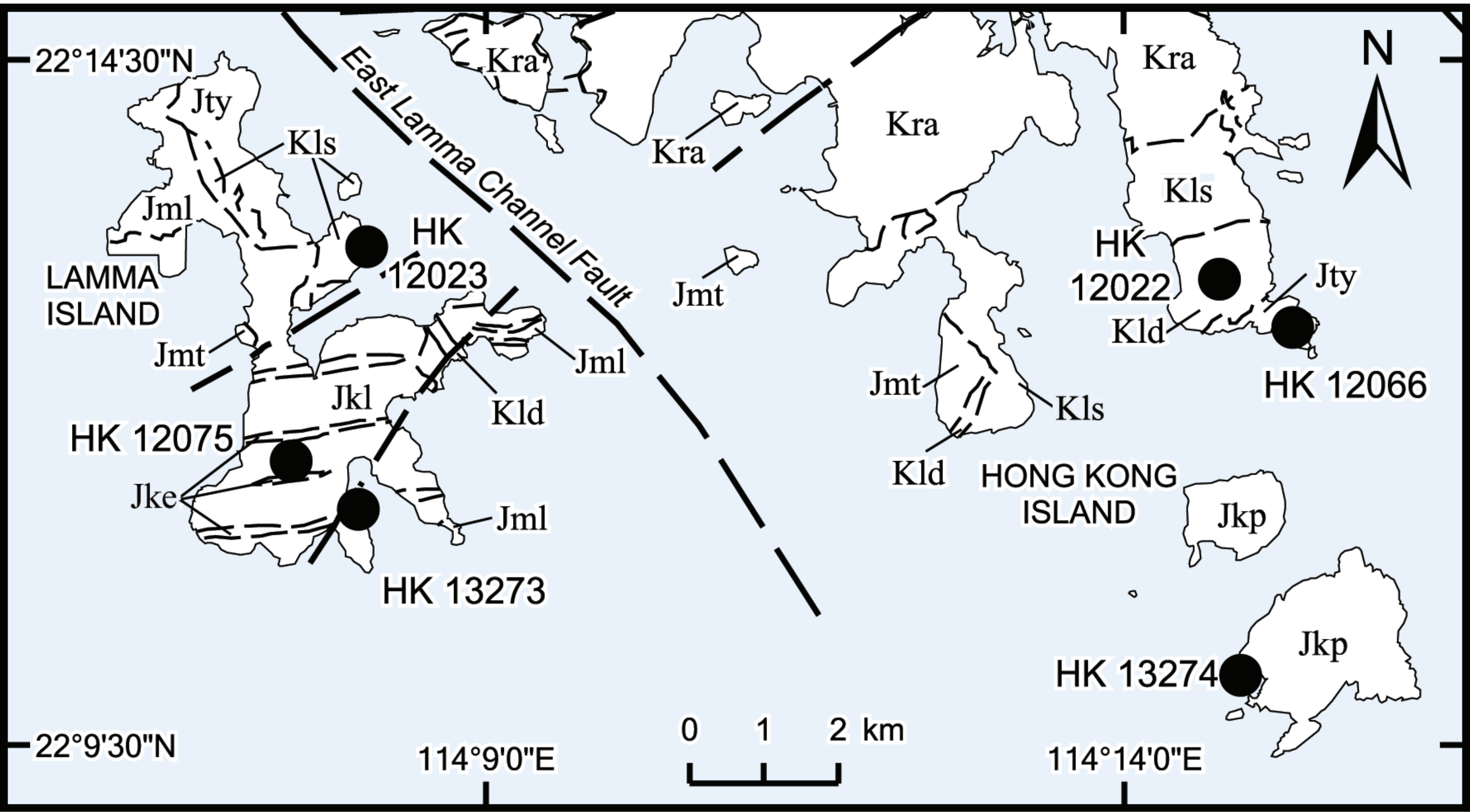

Figure 4 Print Only

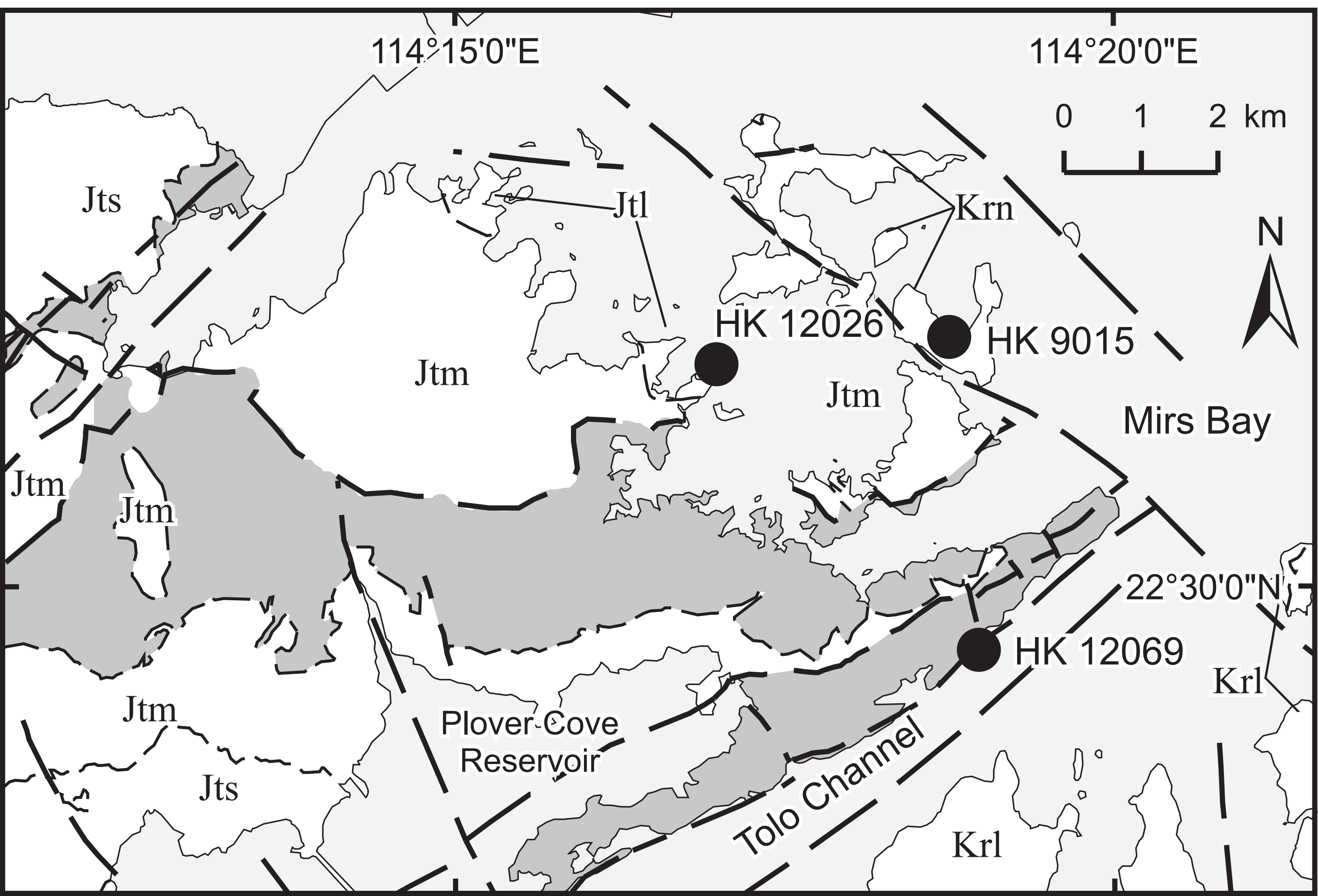

Figure 4 Web Only

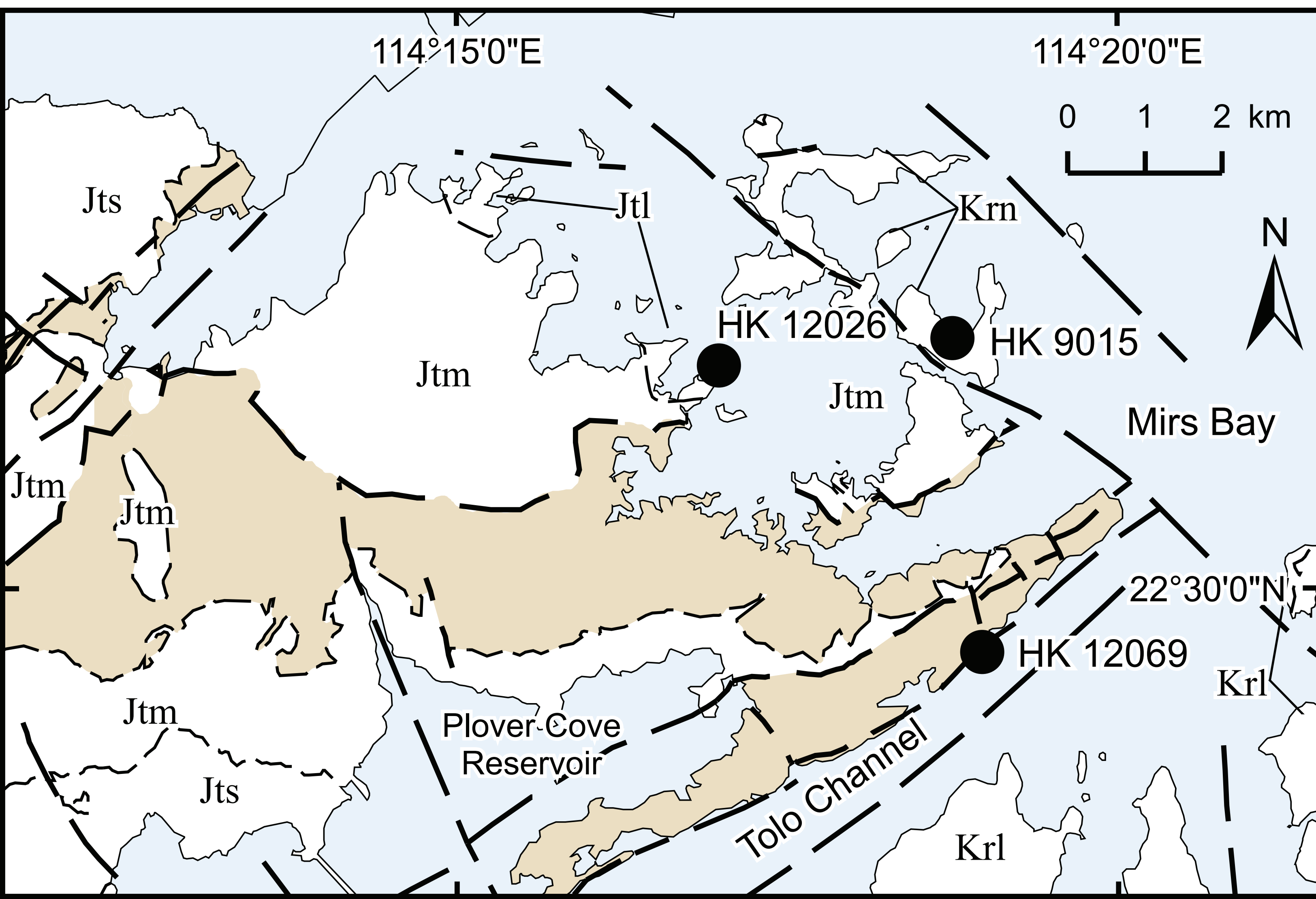

Figure 5 Print Only

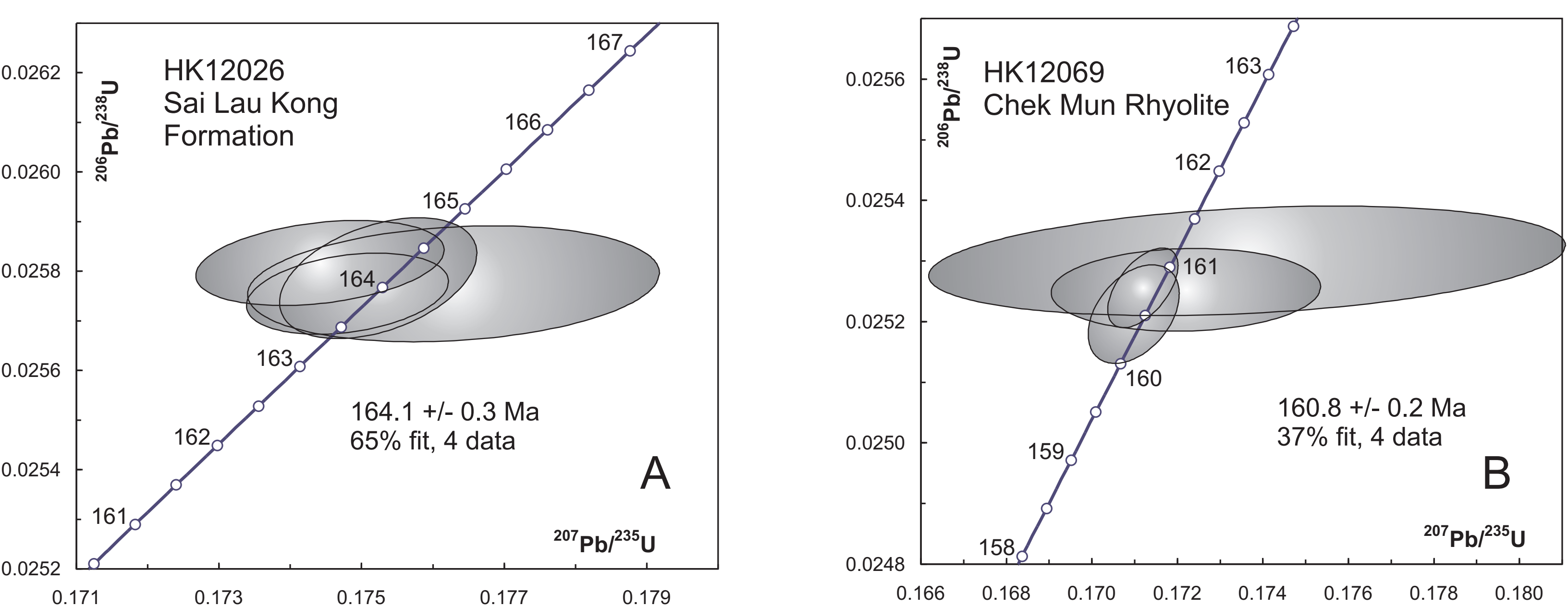

Figure 5 Web Only

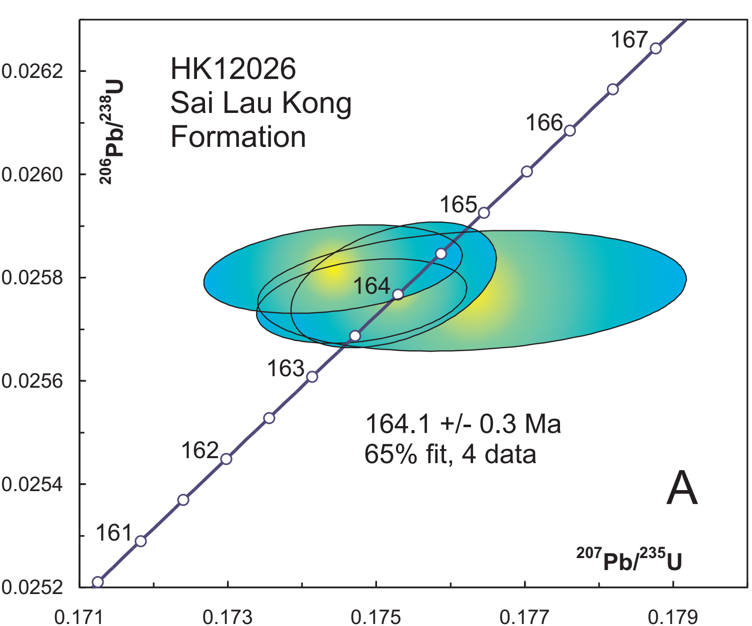

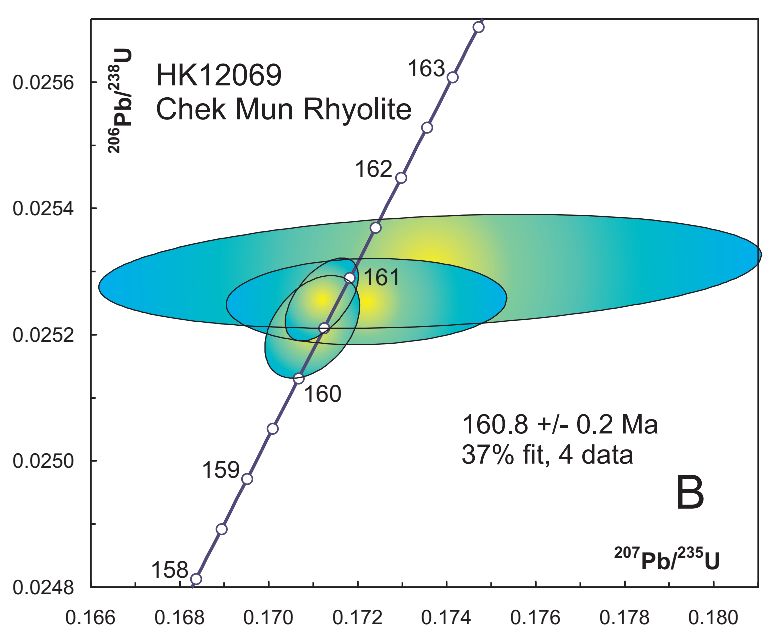

Figure 6 Print Only

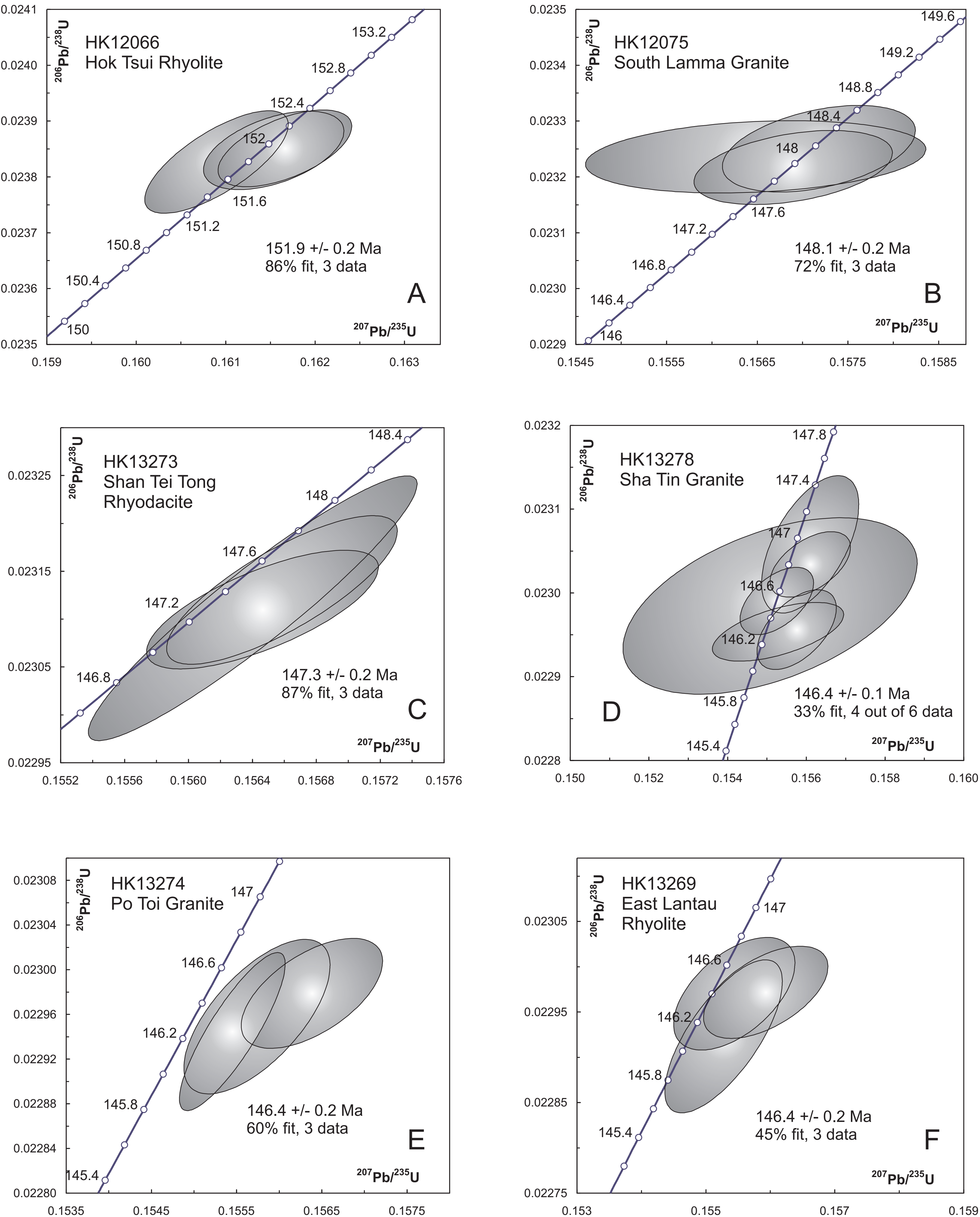

Figure 6 Web Only

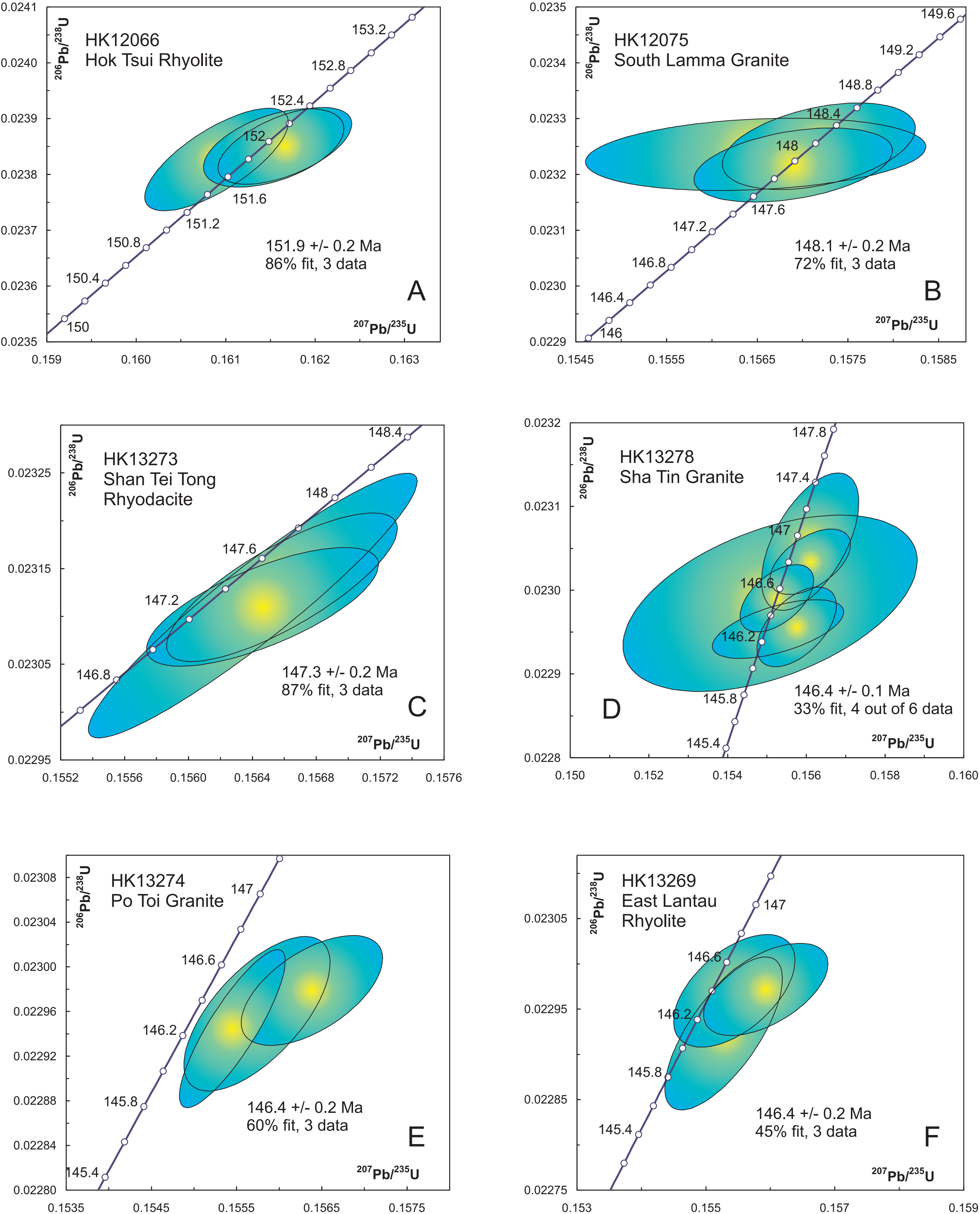

Figure 7 Print Only

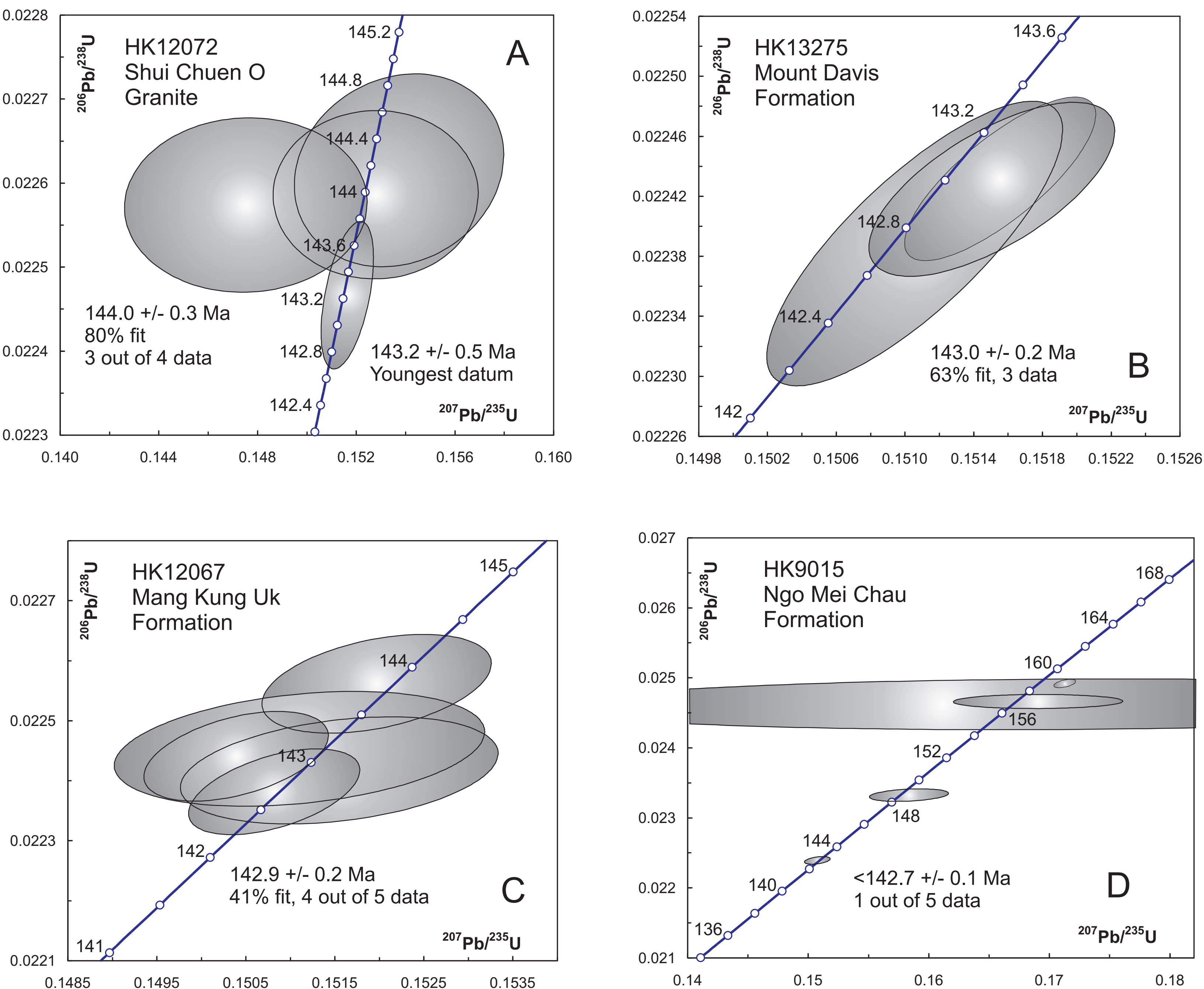

Figure 7 Web Only

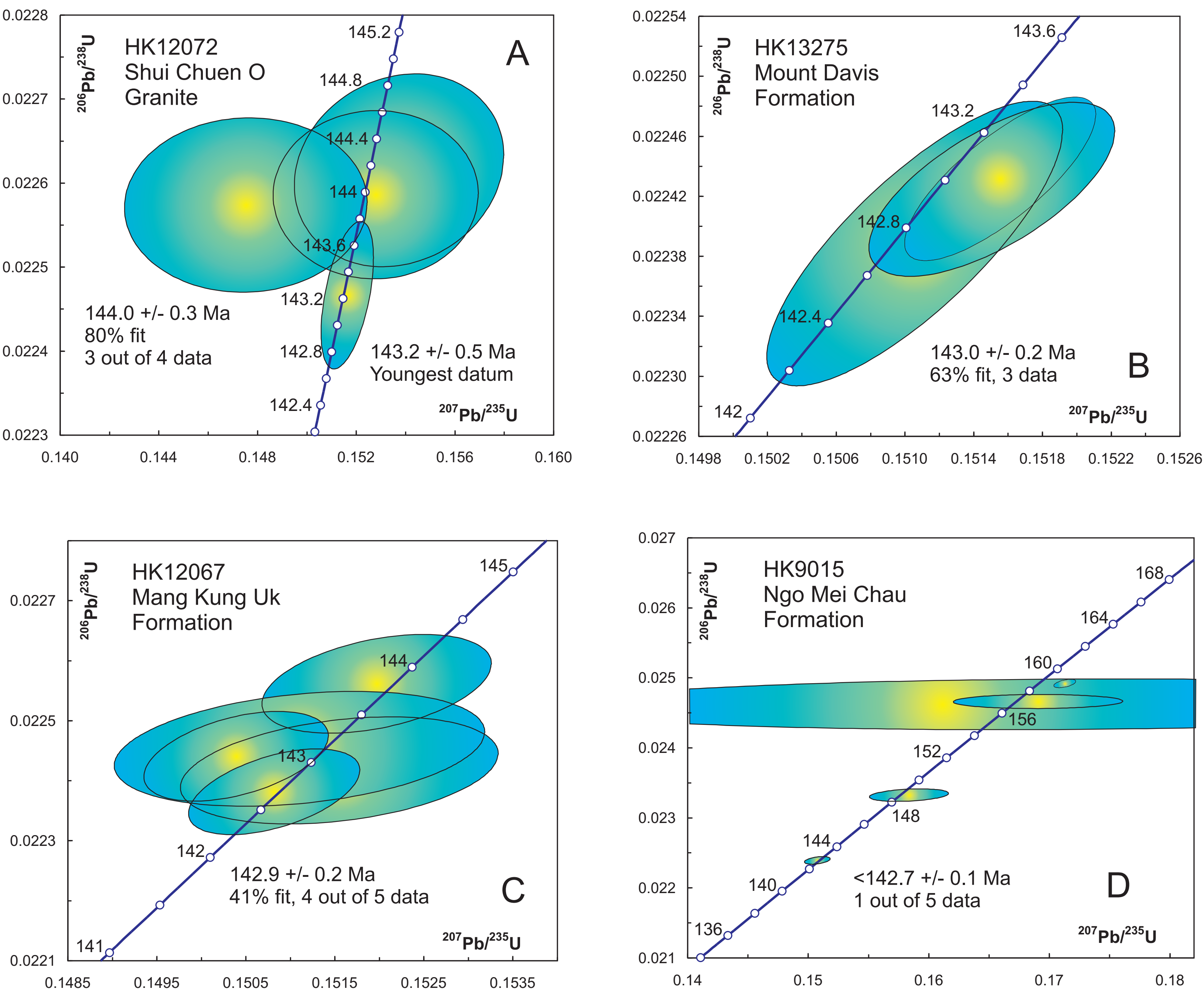

Figure 8 Print Only

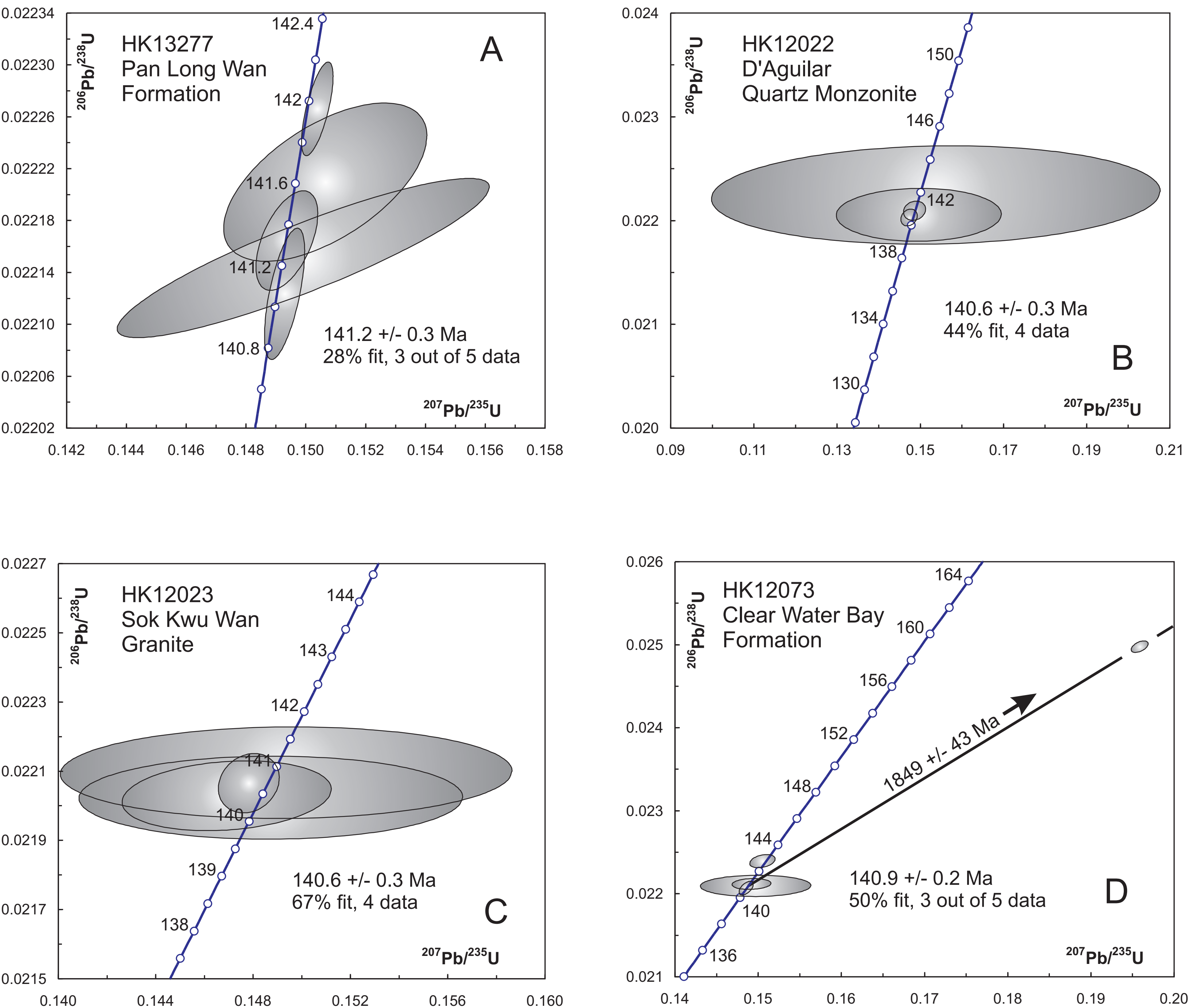

Figure 8 Web Only

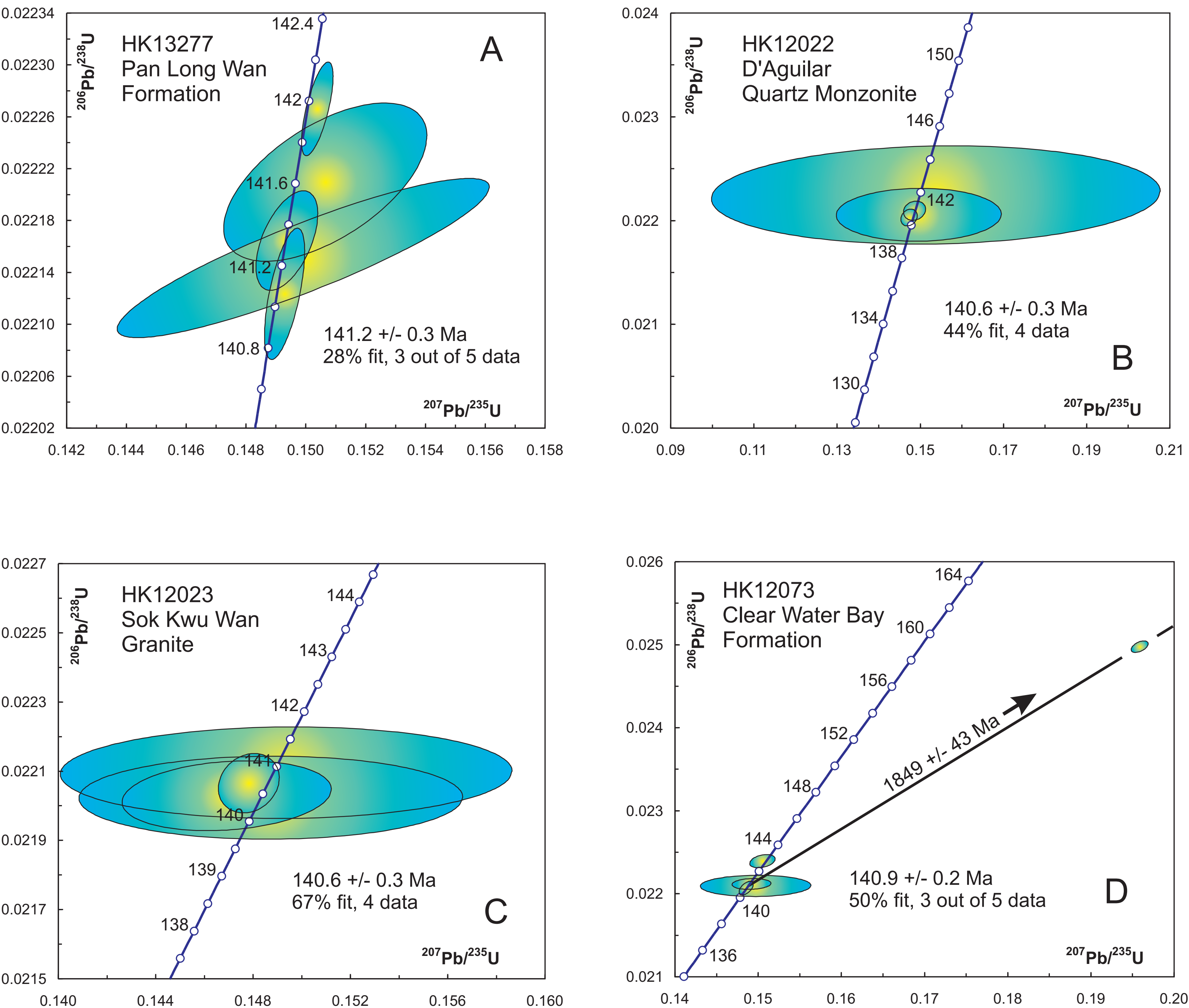

Table 1

Table 1

Locations and descriptions of analyzed samples

Formation/Pluton	Sample	Lat./Long.	Field description	Zircon description
Period 1				
Sai Lau King Formation	HK12026	22º31'31.773, 114º17'10.150	Rhyodacite lava flow, youngest formation of Tsuen Wan Volcanic Group, intercalated with tuff-breccia, tuffaceous sandstone and siltstone. Restricted to Double Haven and Starling Inlet areas.	Small amount of zircon, fresh, euhedral prismatic grains, some with well-developed high order crystal faces.
Chek Mun Rhyolite	HK12069	22º29'30.098, 114º19'06.203	5 m–wide NE-trending quartz phyric rhyolite dyke intruding Tolo Channel Formation at Pak Kok Tsui on N side of Tolo Channel, part of swarm of NE-trending rhyolite dykes across New Territories.	Moderate amount of zircon, long and short prismatic colourless crystals with poorly developed high-order faces, abundant melt inclusions.
Hok Tsui Rhyolite	HK12066	22º11'52.041, 114º15'38.112	10 m–wide NE-trending quartz phyric rhyolite dyke at Hok Tsui, D'Aguilar Peninsula. Part of swarm of NE-trending, flow-banded rhyolite dykes intruding Tai Po Granodiorite and Yim Tim Tsai Formation tuff.	Moderately abundant cracked zircon, colourless short-prismatic grains, high-order crystal faces, abundant amorphous melt inclusions.
Period 2				
South Lamma Granite	HK12075	22º31'26.733, 114º07'36.344	Medium-grained granite. Forms subcircular pluton centred on the southern part of Lamma island. Sample collected from near the summit of Mt Stenhouse, highest point on the island.	Abundant but highly altered zircon, colourless short and long prismatic crystals with well-developed high-order faces.
Shan Tei Tong Rhyodacite	HK13273	22º11'09.999, 114º08'07.768	Rhyodacite core of 40 m-wide composite dyke with basaltic andesite margins exposed in the southern part of Lamma Island. Part of a swarm of E-trending dominantly felsic dykes intruding the South Lamma Granite.	Zircon population similar to HK12075 but more abundant
Sha Tin Granite	HK13278	22º20'52.570, 114º10'08.239	Coarse-grained granite. Forms an NE-oriented pluton centred on Sha Tin. Sample from near the top Beacon Hill. Only sample of Sha Tin Granite to be dated south of the Tolo Channel Fault.	Abundant euhedral prismatic zircon.
Po Toi Granite	HK13274	22º09'50.891, 114º15'03.381	Medium-grained granite. Isolated pluton forming the Po Toi Island Group in SE Hong Kong. From a coastal exposure on Po Toi Island with large angular xenolithic blocks of coarse-grained Lantau Granite.	Small amount of euhedral prismatic zircon, generally altered.
East Lantau Rhyolite	HK13269	22º17'09.967, 114º04'46.796	Feldsparphyric rhyolite dyke. Sampled from a prominent 10 m-wide ENE-trending dyke on the northeastern tip of Kau Yi Chau. Dyke intrudes block of coarse ash crystal tuff. Part of the Lantau Dyke Swarm.	Moderate amount of fresh prismatic zircon with abundant melt inclusions.

Table 1 *(continued)*

Formation/Pluton	Sample	Lat./Long.	Field description	Zircon description
Period 3				
Shui Chuen O Granite	HK12072	22º21’52.089, 114º12’15.394	Medium-grained granite. Forms an ellipsoidal pluton with long axis oriented to northeast on south side of Sha Tin valley. Sample from near the summit of Shui Chuen O.	Small amount of zircon, mostly colourless short-prismatic altered crystals with low-order crystal faces and few inclusions.
Mount Davis Formation	HK13275	22º16’24.329, 114º07’19.053	Coarse ash crystal tuff. Large outcrop of coarse ash tuff with intercalated volcaniclastic sedimentary rocks exposed on northwestern Hong Kong Island. Sample from type locality of the formation at Mount Davis.	Moderate amount of prismatic zircon with melt inclusions.
Mang Kung Uk Formation	HK12067	22º19’10.893, 114º16’45.810	Coarse ash crystal tuff. Dominantly a volcaniclastic unit comprising well-bedded tuffite and epiclastic units and occasional interbedded fine and coarse tuff layers. Sample from near base of formation at Pik Sha Wan.	Small amount of zircon, generally tiny short-prismatic colourless crystals with low-order faces.
Ngo Mei Chau Formation	HK9015	22º31’43.397, 114º18’53.391	Eutaxitic fine ash tuff exposed on Ngo Mei Chau in Mirs Bay. Formation comprises dominantly welded fine ash vitric tuff, with subordinate lapilli tuff and rhyolite lava and is bounded in the west by a NW-trending fault.	Small amount of zircon, euhedral with well-developed low-order crystal faces and melt inclusions, no evidence of cores .
Period 4				
Pan Long Wan Formation	HK13277	22º17’08.173, 114º17’24.671	Trachydacite lava. Forms part of a lava dome overlying the Mang Kung Uk Formation at Clear Water Bay. Thought to represent a final expression of the 142 Ma magmatic event.	Small amount of zircon, high proportion of stubby grains with melt inclusions.
D'Aguilar Quartz Monzonite	HK12022	22º12’43.105, 114º14’51.007	Medium-grained quartz monzonite sampled from a large stock exposed on D’Aguilar Peninsula. Intruded on the northern margin by fine-grained granite correlated with the Sok Kwu Wan pluton	Abundant zircon, fresh, euhedral, prismatic grains with high order crystal faces; large, amorphous melt inclusions.
Sok Kwu Wan Granite	HK12023	22º12’58.095, 114º08’02.499	Fine-grained granite sampled from a pluton centred on the eastern side of Lamma Island in the vicinity of Sok Kwu Wan. Texturally similar to nearby quartz monzonite outcrops but contains more quartz.	Small amount of fresh, euhedral, colourless zircon.
Clear Water Bay Formation	HK12073	22º22’58.217, 114º14’05.068	Feldsparphyric rhyolite lava. Large intrusion of rhyolite lava exhibiting subvertical flow-banding within main vent feeder complex subparallel to the Chek Keng Fault. Sample collected from near Shek Nga Shan.	Abundant colourless short prismatic zircon grains, many with melt inclusions and some with high-order crystal faces.

Table 2

Table 2
U−Pb isotopic data on zircon from Hong Kong rocks

Fraction Analyzed		Weight (mg)	U (ppm)	Th/U	PbC (pg)	$^{206}Pb/^{204}Pb*$	$^{206}Pb†/^{238}U$ Age (Ma)	2σ abs.	$^{207}Pb†/^{235}U$ Age (Ma)	2σ abs.	$^{207}Pb†/^{206}Pb$ Age (Ma)	2σ abs.	Error Correl. Coefficient
HK12026 Sai Lau Kong Formation													
1	3 AB ZR, LPR	0.008	139	0.52	0.7	2603	163.92	0.42	163.57	1.01	158.5	14.9	0.298
2	1 AB ZR	0.004	301	0.67	1.7	1201	164.04	0.60	164.86	2.05	176.5	30.7	0.186
3	3 AB ZR	0.015	73	0.60	0.7	2479	164.31	0.44	163.23	1.24	147.6	18.3	0.302
4	3 AB ZR, INCL	0.012	121	0.50	0.6	3863	164.11	0.63	163.94	0.98	161.4	14.1	0.410
HK12069 Chek Mun Rhyolite													
5	3 AB ZR, EQ, CK	0.010	326	0.65	13.4	413	161.1	0.46	162.6	5.26	184.4	78.3	0.275
6	5 AB ZR, SPR	0.012	241	0.68	0.8	5974	160.8	0.34	160.5	0.58	155.5	7.7	0.553
7	3 AB ZR, LPR, INCL	0.008	380	0.79	5.6	890	160.8	0.35	161.3	2.23	169.5	34.6	0.068
8	3 AB ZR, SPR	0.007	312	0.76	0.9	3909	160.5	0.42	160.3	0.76	156.6	10.9	0.406
HK12066 Hok Tsui Rhyolite													
9	5 AB ZR, CK	0.01	362	0.65	0.7	8338	151.95	0.35	152.16	0.53	155.4	7.2	0.573
10	4 AB ZR, SPR, CK	0.015	341	0.64	1.7	4741	151.93	0.36	152.05	0.56	153.9	8.2	0.490
11	12 AB ZR, SPR	0.02	262	0.68	1.0	8123	151.80	0.47	151.49	0.57	146.7	6.6	0.728
HK12075 South Lamma Granite													
12	4 AB ZR, INCL	0.02	140	0.68	1.1	3821	148.17	0.40	148.23	0.76	149.2	11.9	0.410
13	1 AB ZR, INCL	0.02	95	0.77	1.9	1484	148.08	0.33	147.62	1.34	140.3	22.3	0.208
14	2 AB ZR, INCL	0.02	231	0.68	2.3	2992	147.96	0.34	147.98	0.78	148.4	12.3	0.389
HK13273 Shan Tei Tong Rhyodacite													
15	2 CA ZR, SPR, INCL	0.019	284	0.75	1.7	4793	147.28	0.32	147.60	0.52	152.7	6.4	0.707
16	2 CA ZR, SPR, INCL	0.018	391	0.60	0.6	17133	147.41	0.40	147.71	0.52	152.4	5.5	0.787
17	2 CA ZR, CK, INCL	0.023	358	0.84	1.1	11616	147.29	0.71	147.55	0.74	151.6	4.4	0.937

Table 2 *(continued)*

Fraction Analyzed		Weight (mg)	U (ppm)	Th/U	PbC (pg)	$^{206}Pb/^{204}Pb^*$	$^{206}Pb^\dagger/^{238}U$ Age (Ma)	2σ abs.	$^{207}Pb^\dagger/^{235}U$ Age (Ma)	2σ abs.	$^{207}Pb^\dagger/^{206}Pb$ Age (Ma)	2σ abs.	Error Correl. Coefficient
HK13278 Sha Tin Granite													
18	1 CA ZR, STUBBY	0.006	328	0.76	1.0	3007	146.80	0.20	147.29	0.73	155.1	11.2	0.525
19	2 CA ZR, FRAG	0.008	297	0.67	1.2	3055	146.31	0.24	146.98	0.72	157.7	10.8	0.536
20	2 CA ZR, TIP FRAG	0.005	570	0.68	1.3	3172	146.53	0.21	146.54	0.67	146.6	10.2	0.528
21	1 CA ZR, STUBBY	0.004	407	0.46	0.8	2676	146.96	0.42	147.29	0.89	152.6	12.6	0.572
22	1 CA ZR, STUBBY	0.006	243	0.63	1.4	1537	146.30	0.18	146.56	1.20	150.9	19.1	0.582
23	1 CA ZR, STUBBY	0.004	383	0.72	3.0	693	146.49	0.54	146.39	2.68	144.7	42.9	0.478
HK13274 Po Toi Granite													
24	1 CA ZR, TIP FRAG	0.012	228	0.67	0.8	5087	146.32	0.36	146.96	0.61	157.2	8.0	0.660
25	1 CA ZR, TIP FRAG	0.009	329	0.58	1.2	3877	146.46	0.25	147.53	0.59	164.8	8.4	0.581
26	1 CA ZR, TIP, CK	0.011	1186	0.57	1.4	13308	146.24	0.36	146.71	0.45	154.2	4.0	0.853
HK13269 East Lantau Rhyolite													
27	2 CA ZR, INCL, SPR	0.015	237	0.14	1.3	4042	146.10	0.44	146.55	0.66	153.7	7.9	0.714
28	2 CA ZR, INCL	0.012	446	0.74	1.5	5276	146.40	0.32	146.70	0.68	151.5	9.8	0.541
29	2 CA ZR, SPR, TIP	0.007	279	0.77	1.0	3007	146.41	0.26	147.13	0.69	158.7	10.1	0.555
HK12072 Shui Chuen O Granite													
30	3 AB ZR	0.010	43	0.98	0.9	693	144.16	0.59	145.21	3.05	162.3	51.4	0.156
31	1 AB ZR, INCL, CK	0.010	137	0.96	3.3	628	143.98	0.52	144.38	2.99	151.0	51.9	0.010
32	1 AB ZR, INCL	0.005	90	0.83	1.2	588	143.90	0.53	139.73	3.56	69.3	64.1	0.028
33	4 AB ZR	0.012	330	0.71	1.8	3109	143.23	0.45	143.36	0.77	145.6	11.6	0.503
HK13275 Mount Davis Formation													
34	1 CA ZR, INCL	0.021	155	0.72	0.8	5562	142.96	0.30	143.24	0.52	147.8	6.9	0.667
35	3 CA ZR, SPR, INCL	0.027	317	0.73	1.4	8811	143.01	0.28	143.28	0.40	147.8	4.5	0.786
36	1 CA ZR, SPR	0.030	153	0.72	1.0	6603	142.73	0.49	142.84	0.62	144.6	6.7	0.795

Table 2 *(continued)*

Fraction Analyzed		Weight (mg)	U (ppm)	Th/U	PbC (pg)	$^{206}Pb/^{204}Pb^{*}$	$^{206}Pb^{\dagger}/^{238}U$ Age (Ma)	2σ abs.	$^{207}Pb^{\dagger}/^{235}U$ Age (Ma)	2σ abs.	$^{207}Pb^{\dagger}/^{206}Pb$ Age (Ma)	2σ abs.	Error Correl. Coefficient
HK12067 Mang Kung Uk Formation													
37	5 AB ZR	0.010	113	0.63	0.6	2768	143.82	0.42	143.64	0.93	140.6	14.9	0.407
38	4 AB ZR, INCL	0.010	195	0.62	2.2	1301	143.14	0.50	142.87	1.51	138.5	25.2	0.294
39	7 AB ZR CK	0.015	128	0.67	0.8	3640	143.06	0.39	142.24	0.75	128.7	11.8	0.457
40	3 ABE ZR, INCL	0.010	251	0.79	1.8	1976	142.91	0.46	143.27	1.29	149.2	21.4	0.317
41	2 AB ZR	0.008	237	0.70	0.6	4570	142.69	0.37	142.62	0.70	141.6	10.6	0.503
HK9015 Ngo Mei Chau Formation													
42	3 AB ZR	0.008	415	0.67	1.5	3121.7	142.69	0.28	142.46	0.77	138.7	12.3	0.416
43	1 AB ZR	0.010	246	0.40	2.5	1483.1	148.58	0.47	149.20	2.36	159.0	38.0	0.282
44	2 AB ZR	0.010	519	0.66	29.3	296.1	157.06	0.51	158.56	5.01	181.0	78.0	0.042
45	17 AB ZR	0.015	477	0.52	3.0	3856.4	158.68	0.31	160.50	0.64	187.4	8.6	0.540
46	4 AB ZR	0.014	325	0.68	123.6	76.08	156.80	1.87	160.12	29.71	209.6	412.0	0.115
HK13277 Pan Long Wan Formation													
47	1 CA ZR, TIP, INCL	0.033	33	0.90	2.2	728	141.60	0.31	142.51	2.44	157.6	40.4	0.586
48	1 CA ZR, TIP	0.043	12	0.66	1.8	400	141.24	0.32	141.86	4.47	152.3	75.2	0.890
49	2 CA ZR, LPR	0.041	41	0.78	0.9	2606	141.32	0.20	141.37	0.74	142.3	11.8	0.532
50	1 CA ZR, LPR, INCL	0.018	97	0.82	0.4	6437	141.06	0.26	141.31	0.49	145.5	6.7	0.645
51	4 CA ZR, LPR, FRAG	0.035	76	0.68	0.5	7032	141.96	0.19	142.28	0.38	147.5	5.0	0.691
HK12022 D'Aguilar Quartz Monzonite													
52	3 AB ZR, INCL	0.015	100.3	0.1	1.45	1481.1	140.44	0.42	139.58	1.40	125.0	24.6	0.210
53	1 AB ZR	0.006	39.9	0.82	2.56	150.6	140.61	1.32	141.66	14.16	159.3	235.0	0.020
54	1 AB ZR	0.025	47.1	0.74	1.62	1050.1	140.86	0.48	140.74	1.94	138.8	34.0	0.158
55	1 AB ZR	0.004	103.6	0.81	13.66	61.535	141.81	2.44	145.23	38.00	201.3	555.0	0.076

Table 2 *(continued)*

Fraction Analyzed		Weight (mg)	U (ppm)	Th/U	PbC (pg)	^{206}Pb / ^{204}Pb*	^{206}Pb† / ^{238}U Age (Ma)	2σ abs.	^{207}Pb† / ^{235}U Age (Ma)	2σ abs.	^{207}Pb† / ^{206}Pb Age (Ma)	2σ abs.	Error Correl. Coefficient
HK12023 Sok Kwu Wan Granite													
56	1 AB ZR	0.003	151.8	0.67	1.88	361	140.42	0.62	140.79	5.66	147.1	98.5	0.013
57	1 AB ZR, LPR	0.008	67.3	0.67	1.12	700	140.46	0.52	139.18	3.10	117.5	54.4	0.186
58	2 AB ZR, INCL	0.008	142.3	0.56	0.68	2378	140.69	0.44	139.98	0.90	119.5	25.0	0.174
59	1 AB ZR	0.003	245	0.5	3.94	283	140.88	0.68	141.35	6.66	154.9	109.0	0.033
HK12073 Clear Water Bay Formation													
60	3 AB ZR, INCL	0.015	217	0.60	1.5	3513	159.00	0.36	181.56	0.70	486.3	8.0	0.507
61	1 AB ZR, ROD INCL	0.010	125	0.47	1.0	1878	142.73	0.41	142.43	1.11	137.5	18.4	0.333
62	1 AB ZR, ROD INCL	0.015	276	0.47	5.7	1056	141.01	0.34	141.31	1.69	146.3	29.6	0.120
63	3 AB ZR, ROD INCL	0.012	537	0.77	25.6	375	140.86	0.65	141.71	4.78	155.9	83.0	0.037
64	2 AB ZR, ROD INCL	0.015	577	0.61	2.8	4424	140.69	0.43	140.71	0.62	141.0	9.3	0.552

Footnotes to Table 2:

Weights are based on estimates from microphotographs.

Abbreviations: Number of grains analyzed is at beginning, AB - air abraded, CA - chemically abraded, ZR - zircon, INCL - inclusions, EQ - equant, SPR - short prismatic, LPR - long prismatic, CK - cracked.

Th/U calculated from radiogenic 208Pb/206Pb ratio and 206Pb/238U age assuming concordance.

PbC: common Pb assuming the isotopic composition of lab blank:
$^{206}Pb/^{204}Pb$ - 18.221; $^{207}Pb/^{204}Pb$ - 15.612; $^{208}Pb/^{204}Pb$ - 39.360 (2% error).

* $^{206}Pb/^{204}Pb$ are measured values corrected for fractionation and spike.

† $^{206}Pb/^{238}U$ age, $^{207}Pb/^{235}U$ age and $^{207}Pb/^{206}Pb$ age are corrected for common Pb assuming laboratory blank composition and 230Th disequilibrium assuming a magmatic Th/U of 4.2.

Uranium decay constants: L238 = 1.55125 X 10^{-4}/Ma, L235 = 938485 X 10^{-4}/Ma (Jaffey et al., 1971).
Concordia coordinates: Y = 206Pb/238U = EXP(L238*(206-238 Age)) - 1; X = 207Pb/235U = EXP(L235*(207-235 Age)) - 1
207Pb/206Pb = X/(137.88*Y);

Error Correl. Coefficient: Error correlation coefficient for concordia coordinates

Table 3

Table 3

Summary of the volcanic–plutonic nomenclature and U–Pb age data for Mesozoic igneous rocks of Hong Kong (after Sewell et al., 2000) [1,2]

VOLCANIC ROCKS				GRANITOID ROCKS			
Group		**Formation**	**U–Pb Age (Ma)**	**Suite**		**Intrusion**	**U–Pb Age (Ma)**
KAU SAI CHAU VOLCANIC GROUP		High Island (Kkh)	140.9 ± 0.2[1]	**LION ROCK SUITE**	'GRANITIC' SUBSUITE	Mount Butler Granite (Klb)	
		Clear Water Bay (Kkw)	140.7 ± 0.2[1]			Kowloon Granite (Klk)	140.4 ± 0.2[1]
			140.9 ± 0.2*			Fan Lau Granite (Kll)	
		Undifferentiated (Kku)	141.1 ± 0.2[2]			Sok Kwu Wan Granite (Kls)	140.6 ± 0.3*
		Pan Long Wan (Kkp)	141.2 ± 0.3*				
					'MONZONITIC' SUBSUITE	Tei Tong Tsui Quartz Monzonite (Klt)	
						Tong Fuk Quartz Monzonite (Klf)	140.4 ± 0.3[1]
						D'Aguilar Quartz Monzonite (Kld)	140.6 ± 0.3*
		Unconformity					
REPULSE BAY VOLCANIC GROUP	'RHYOLITIC' SUBGROUP	Mount Davis (Krd)	142.8 ± 0.2[2]	**CHEUNG CHAU SUITE**			
			143.0 ± 0.2*				
		Long Harbour (Krl)	142.7 ± 0.2[1]				
			142.8 ± 0.2[1]				
						Luk Keng Quartz Monzonite (Kcl)	
						Chi Ma Wan Granite (Kcc)	<143.7 ± 0.3[1]
	'TRACHYTIC' SUBGROUP	Mang Kung Uk (Krm)	142.9 ± 0.2*			Shui Chuen O Granite (Kcs)	144.0 ± 0.3*
		Che Kwu Shan (Krc)	142.5 ± 0.3[1]				
		Ap Lei Chau (Kra)	142.7 ± 0.2[1]				
		Ngo Mei Chau (Krn)	<142.7 ± 0.1*				
		Unconformity					
LANTAU VOLCANIC GROUP				**KWAI CHUNG SUITE**		Sha Tin Granite (Jkt)	146.4 ± 0.1*
							146.2 ± 0.2[1]
						East Lantau Rhyolite (Jko)	146.3 ± 0.3[1]
		Lai Chi Chong (Jll)	146.6 ± 0.2[2]				146.4 ± 0.2*
		Undifferentiated (Jlu)	146.6 ± 0.2[1]			East Lantau Rhyodacite (Jkd)	146.5 ± 0.2[1]
		Undifferentiated (Jlu)	147.5 ± 0.2[2]			Needle Hill Granite (Jkn)	146.4 ± 0.2[1]
						Sham Chung Rhyolite (Jks)	146.6 ± 0.2[2]
						Po Toi Granite (Jkp)	146.4 ± 0.2*
						Shan Tei Tong Rhyodacite (Jke)	147.3 ± 0.2*
						South Lamma Granite (Jkl)	148.1 ± 0.2*
						Hok Tsui Rhyolite	151.9 ± 0.2*
		Unconformity					
TSUEN WAN VOLCANIC GROUP				**LAMMA SUITE**	'A-TYPE' SUBSUITE	Tai Lam Granite (Jma)	159.3 ± 0.3[1]
						Tsing Shan Granite (Jms)	<159.6 ± 0.5[1]
						Chek Lap Kok Granite (Jmc)	160.4 ± 0.3[1]
						Chek Mun Rhyolite	160.8 ± 0.2*
		Sai Lau Kong (Jtl)	164.1 ± 0.3*		'I-TYPE' SUBSUITE		
		Tai Mo Shan (Jtm)	<164.5 ± 0.7[1]				
		Shing Mun (Jts)	164.2 ± 0.3[2]			Lantau Granite (Jml)	161.5 ± 0.2[1]
			164.7 ± 0.3[2]			Tai Po Granodiorite (Jmt)	<164.6 ± 0.2[1]
		Yim Tin Tsai (Jty)	164.5 ± 0.2[1]				

[1] U–Pb ages from Davis et al. (1997). [2] U–Pb ages from Campbell et al. (2007). * This paper.